高温超伝導の理論的研究

柳澤孝[1], 宮崎真長[2], 山地邦彦[1]

[1] National Institute of Advanced Industrial Science and Technology (AIST)
[2] Hakodate National College of Technology

Outline

1. Introduction
2. Superconductivity
3. High Temperature Superconductivity
4. Hubbard Model
5. Variational Monte Carlo method
6. Stripes in high-Tc cuprates
7. Spin-orbit coupling and Lattice distortion
8. Summary

1. Introduction

Key words: Physics from U (Coulomb interactions)

- A possibility of superconductivity
  Superconductivity from U
- Competition of AF and SC
- Incommensurate state
  Stripes and SC
  Compete and Collaborate
- Stripes in the lightly-doped region
- Singular Spectral function

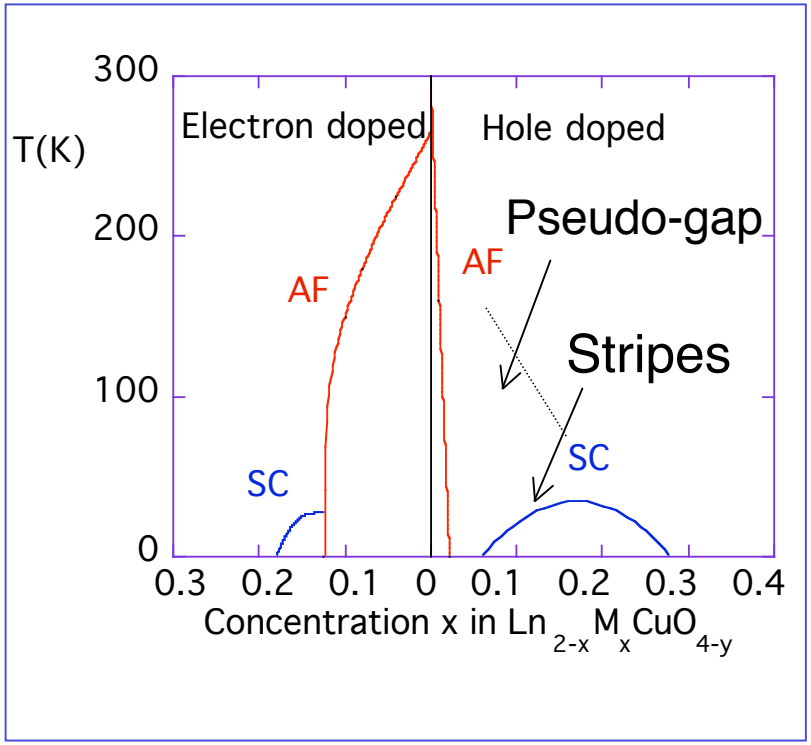

Purpose of Theoretical study

1. Origin of the superconductivity
   - Symmetry of Cooper pairs
   - Mechanism of attractive interaction

     Coulomb interaction U, Exchange interaction J

2. Physics of Anomalous Metallic behavior
   - Inhomogeneous electronic states: stripe
   - Pseudogap phenomena
   - Structural transition LTO, LTT

2. Superconductivity

1911 Kamerlingh Onnes

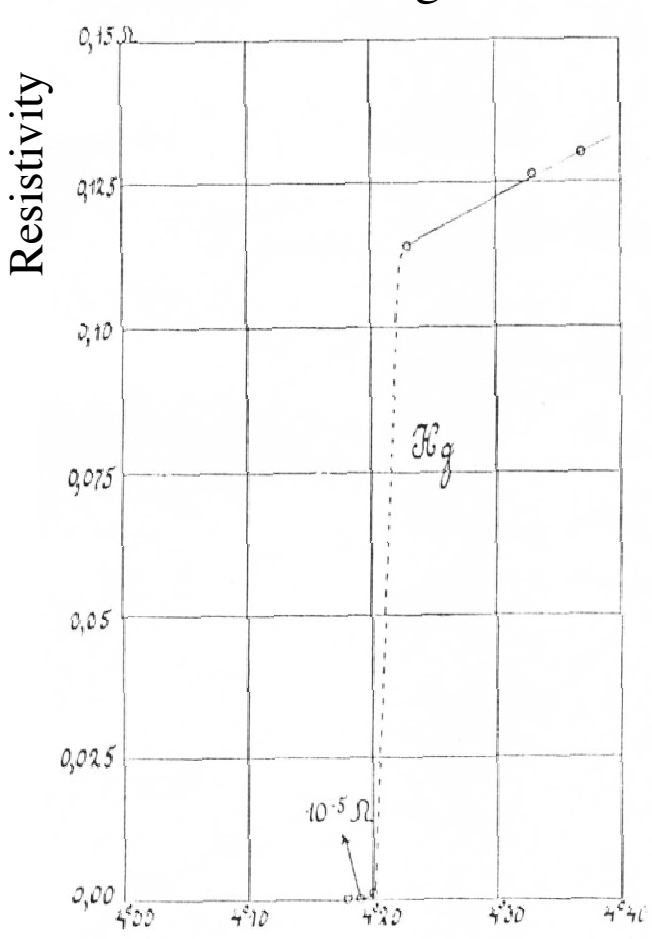

Elements that become superconducting

Superconductive at low temperatures

Superconductive under pressure

巨視的量子現象

kと-kの電子がペアーをつくり、ゲージ（位相）不変性が破れた状態

電子には位相という仮想的空間内での回転の自由度があり、勝手な方向を向いている。が、超伝導状態ではすべての電子ペアが同じ方向を向いている。

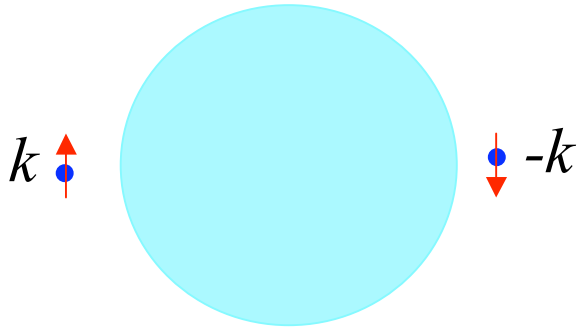

対称性の破れ

BCS理論

引力相互作用によるフェルミ面の不安定性によって超伝導がひきおこされる

超伝導体の特徴

電気抵抗 0

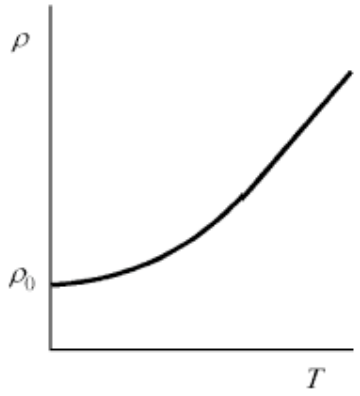

金属

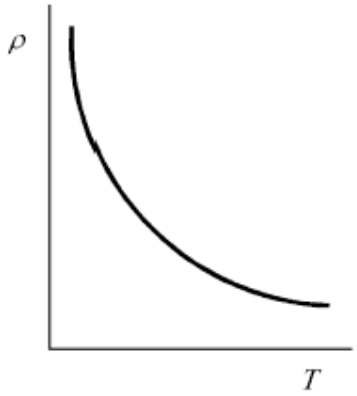

半導体

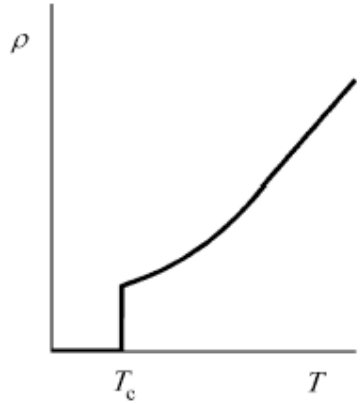

超伝導体

マイスナー効果

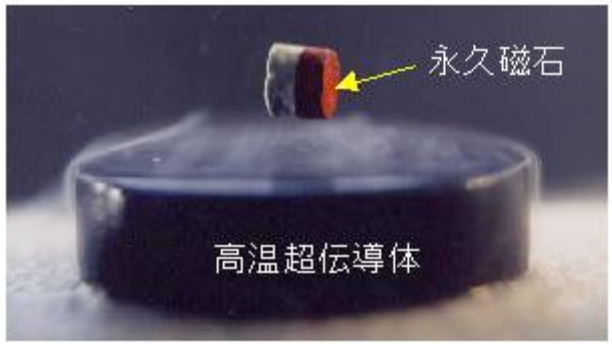

磁場は超伝導体に入り込むことができない

フッシング効果　超伝導体に磁石を近付けておいて冷やすと超伝導体内部に入り込んだ磁場により（第２種超伝導体）、つりあげることができる。

BCS理論

BCS理論　どうして電子対を考えたか　（近藤淳「超伝導」（固体物理）より）

超伝導状態：　一つのSlater行列式では表わせない

電子間引力　H_1

$H = H_0 + H_1$　　$\Psi = \sum_j c_j \Psi_j$　　Ψ_j : Slater行列式

Ψ_0 : Fermi球

波動関数　$\Psi = c_0 \Psi + \sum_{j \neq 0} c_j \Psi_j$　　摂動計算　$c_0 \approx 1$

$c_j \langle \Psi_0 H_1 \Psi_j \rangle < 0$

エネルギー　$\langle \Psi H \Psi \rangle = \sum c_j^2 \langle \Psi_j H_0 \Psi_j \rangle + \sum c_i c_j \langle \Psi_i H_1 \Psi_j \rangle$

もし、すべての $\langle \Psi_i H_1 \Psi_j \rangle < 0$　なら、すべての $c_j > 0$

Ψ_jとしてペアーの状態をとるならば、c_j>0として
エネルギーを下げることができる。

BCS波動関数

電子対 $\Psi_i = \left| k_1 \uparrow -k_1 \downarrow, k_2 \uparrow -k_2 \downarrow, k_3 \uparrow -k_3 \downarrow, \right\rangle$

$\Psi_j = \left| k'_1 \uparrow - k'_1 \downarrow, k_2 \uparrow -k_2 \downarrow, k_3 \uparrow -k_3 \downarrow, \right\rangle$

順番を変えても
符号は変わらない。

$$\left\langle \Psi_i H_1 \Psi_j \right\rangle = \left\langle k'_1 -k'_1 | V | k_1 - k_1 \right\rangle < 0$$

非対角要素を常に負にできる

基底状態はすべての対状態の一次結合で表わされる:

$$\Psi = \sum c_{k_1 k_2} \left| k_1 \uparrow -k_1 \downarrow, k_2 \uparrow -k_2 \downarrow, \right\rangle$$

独立対近似（一体近似）をすると

$$\Psi = \sum c_{k_1} c_{k_2} \left| k_1 \uparrow -k_1 \downarrow, k_2 \uparrow -k_2 \downarrow, \right\rangle$$

N電子項のみを取り出すとして

$$\Phi = \prod_k \left(u_k + v_k \left| k \uparrow -k \downarrow \right\rangle \right)$$

BCSの波動関数

$$\frac{\sqrt{\left(N - \langle N \rangle\right)^2}}{\langle N \rangle} \propto \frac{1}{\sqrt{\langle N \rangle}}$$

粒子数のゆらぎは小さい

3. 高温超伝導

超伝導臨界温度

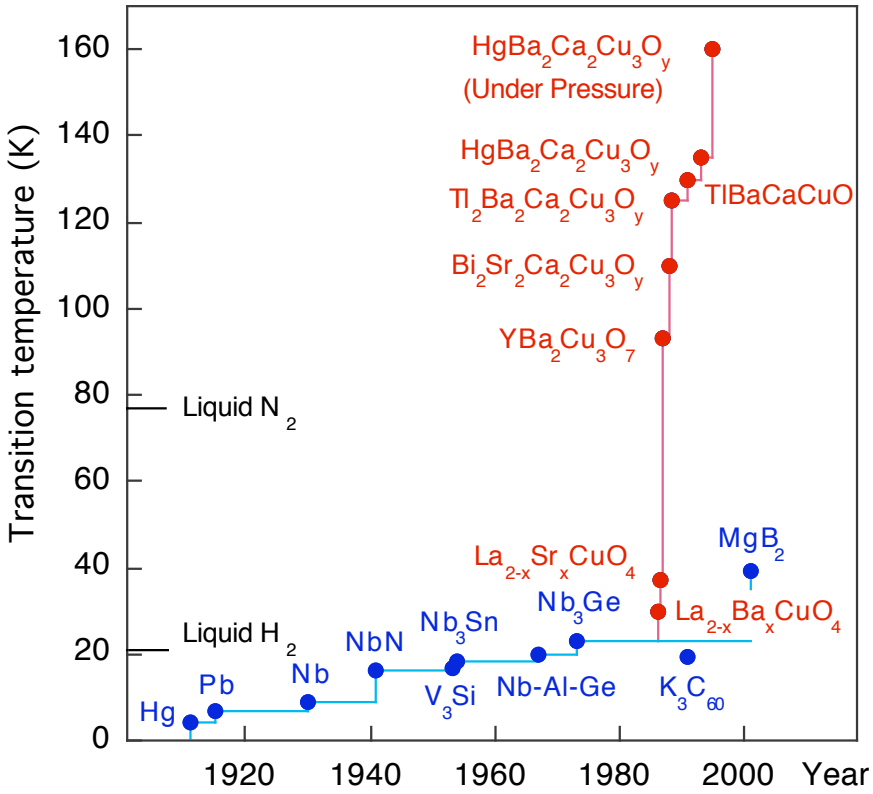

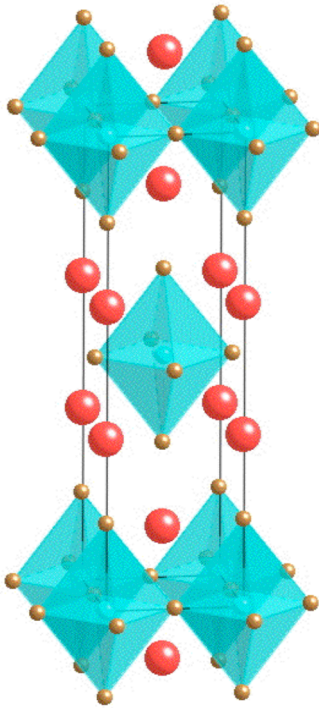

La_2CuO_4

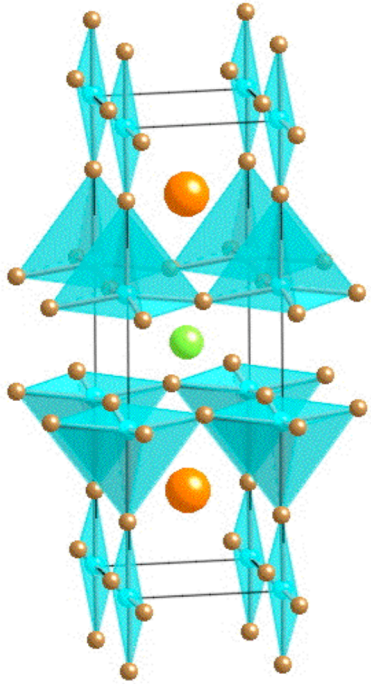

$YBa_2Cu_3O_7$

高温超伝導体の相図

高温超伝導体の相図

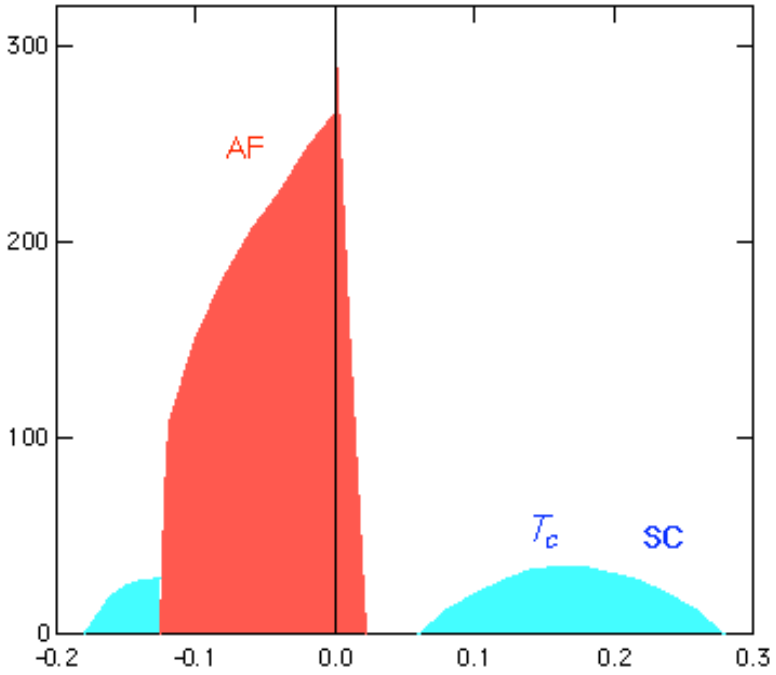

ホール数　　電子キャリアー数

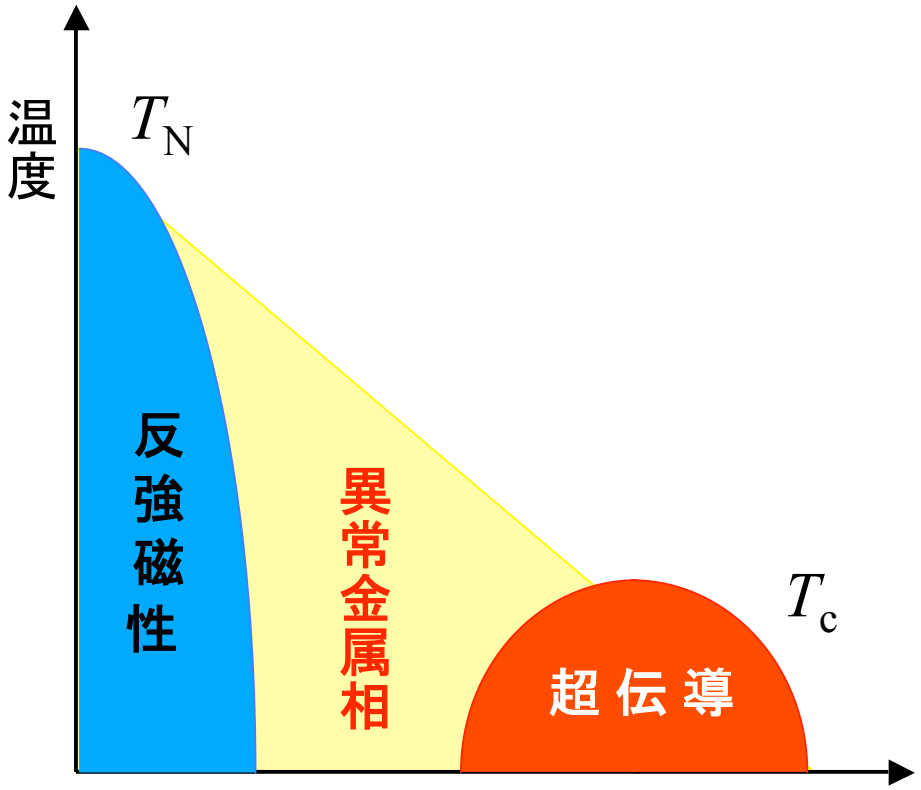

キャリアー数

高温超伝導体のモデル

銅と酸素を含む二次元面

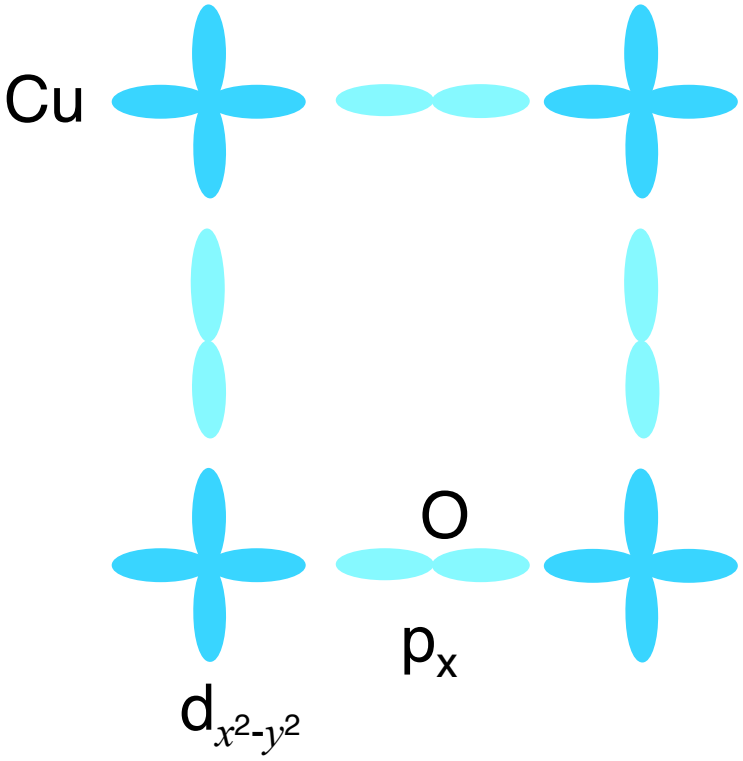

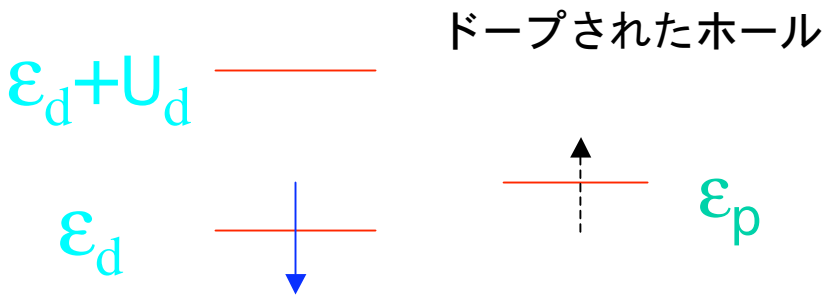

銅酸化物の特徴

- 二次元的である
- スピンが1/2（小さい）
- 銅，酸素のhole levelが近い

電気抵抗の温度依存性

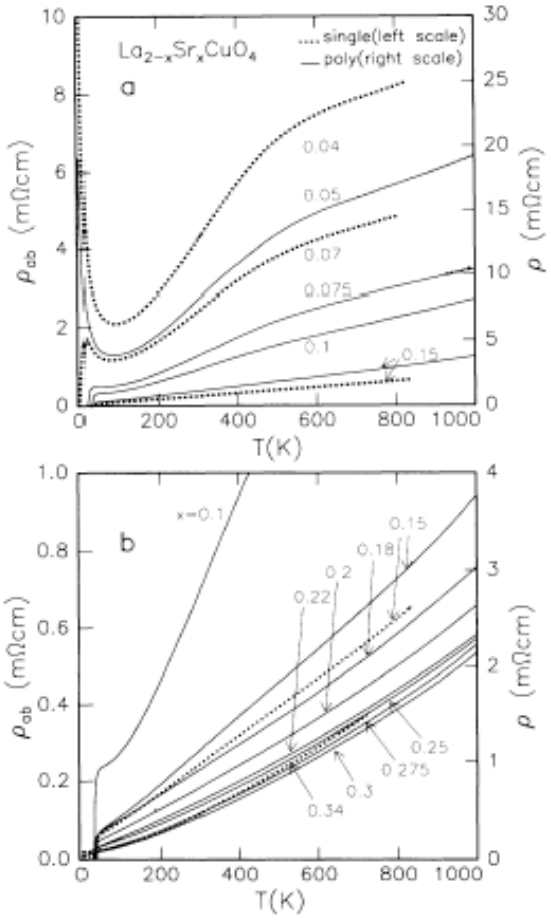

FIG. 1. The temperature dependence of the resistivity for $La_{2-x}Sr_xCuO_4$. (a) $0 < x \leq 0.15$, (b) $0.1 \leq x < 0.35$. Dotted lines, the in-plane resistivity (ρ_{ab}) of single-crystal films with (001) orientation; solid lines, the resistivity (ρ) of polycrystalline materials. Note, $\rho_M = (h/e^2)d = 1.7$ mΩ cm.

H. Takagi et al.

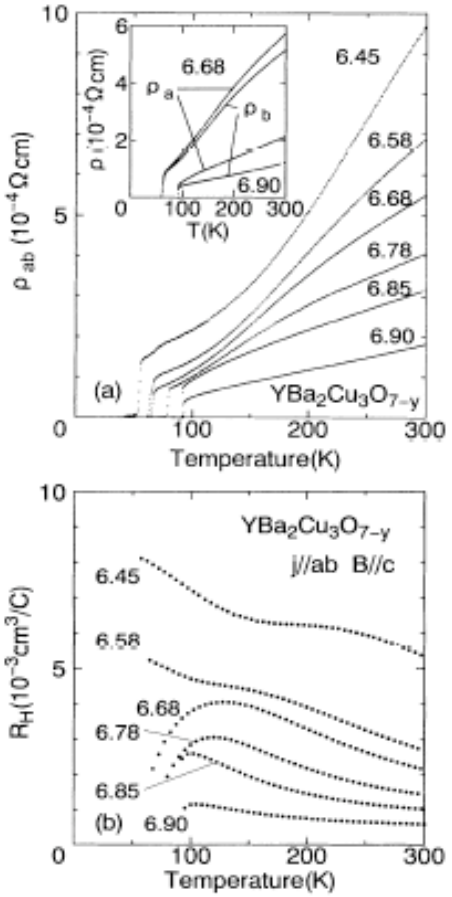

FIG. 1. (a) Temperature dependence of in-plane resistivity of twinned $YBa_2Cu_3O_{7-y}$ crystals with oxygen concentration $7-y$ ~6.90, 6.85, 6.78, 6.68, 6.58, and 6.45. Inset: Temperature dependence of ρ_a and ρ_b for detwinned crystals of T_c=90 and 60 K. (b) Temperature dependence of R_H of twinned crystals measured under $\mathbf{j} \parallel ab$ plane and $\mathbf{B} \parallel c$ axis at $B = 5$ T.

T. Ito et al.

比 熱

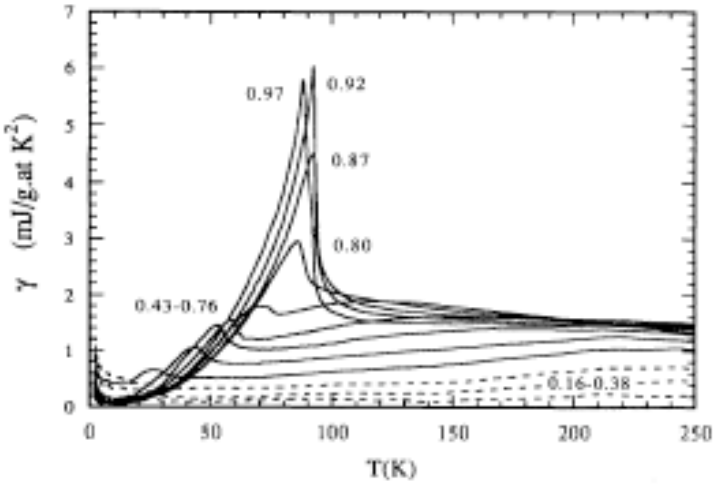

FIG. 4. Electronic specific heat coefficient $\gamma(x,T)$ vs T for $YBa_2Cu_3O_{6+x}$ relative to $YBa_2Cu_3O_6$. Values of x are 0.16, 0.29, 0.38, 0.43, 0.48, 0.57, 0.67, 0.76, 0.80, 0.87, 0.92, and 0.97.

Loram et al., Phys. Rev. Lett. 71, 1740 (1993)

LSCO

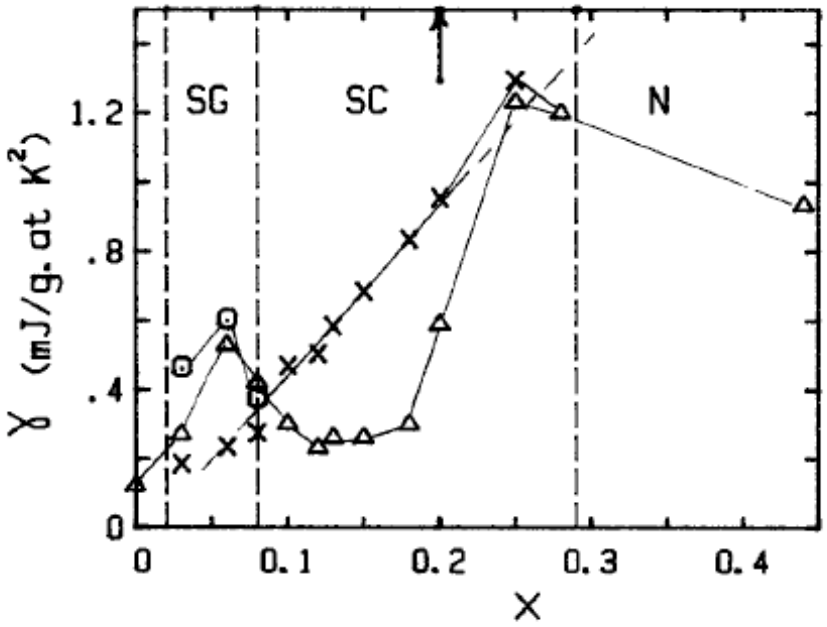

FIGURE 2

γ vs x. for x≤.08 Δ,γ(2K); o,γ(8K); x,γ(40K)
for x≥.1 Δ,γ(0); x, γ_n

Loram et al., Physica C162-164, 498 (1989)

磁気緩和率

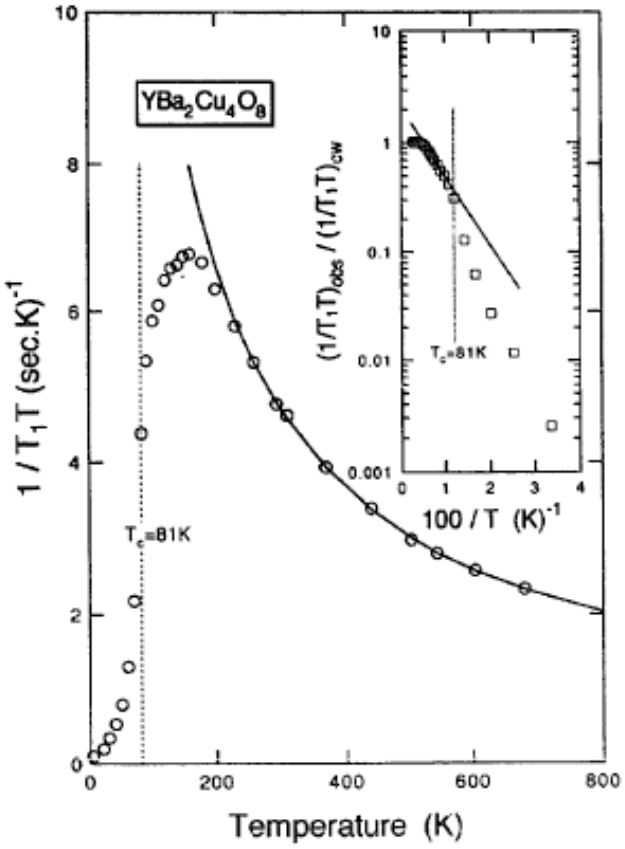

Fig. 1. Temperature dependence of the nuclear spin–lattice relaxation rate $1/T_1T$ for Cu(2) sites of $YBa_2Cu_4O_8$. The solid curve shows the best fit of the data to Eq. (1) for $T > 250$ K. The inset shows the Arrhenius plots for the ratio of the observed $(1/T_1T)_{obs}$ to the expected $(1/T_1T)_{cw}$ from Eq. (1), and the best fit of the data to Eq. (2) is shown by the solid line.

Yasuoka et al., Physica B199 (1994)278

$YBa_2Cu_4O_8$

アンダードープ域　T_c= 81K

Tcより上の温度から帯磁率が下がりはじめる。

擬ギャップ

スピンゆらぎ理論によると

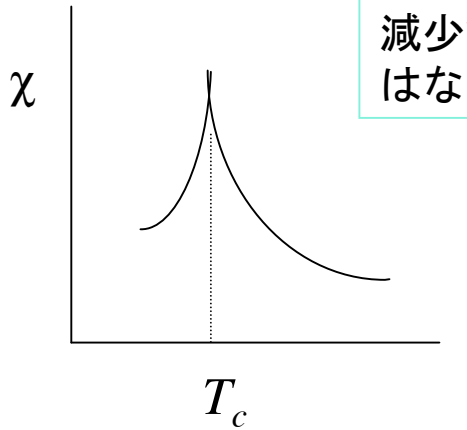

Tcより上から減少することはない。

量子臨界現象

量子相転移

- T= 0で起こる相転移
- 量子ゆらぎが重要

  量子ゆらぎにより引きおこされる
- 圧力、磁場変化、元素置換等による相転移
- 量子臨界点（相転移点）の近くでは非フェルミ流体の振る舞いが見られることがある。

  抵抗、比熱、帯磁率

スピンゆらぎ理論（Millis, Moriya）

3D	C/T	$\chi(Q)$	ρ	χ_s
Ferro.	-lnT	$T^{-4/3}$	$T^{5/3}$	$T^{-4/3}$
AF	$T^{1/2}$	$T^{-3/2}$	$T^{3/2}$	$T^{-3/4}$

2 D	C/T	$\chi(Q)$	ρ	χ_s
Ferro.	$T^{-1/3}$	$(T\ln T)^{-1}$	$T^{4/3}$	$\chi(Q)^{3/2}$
AF	-lnT	T^{-1}	T	T^{-1}

4. Hubbard Model

Itinerant Electrons

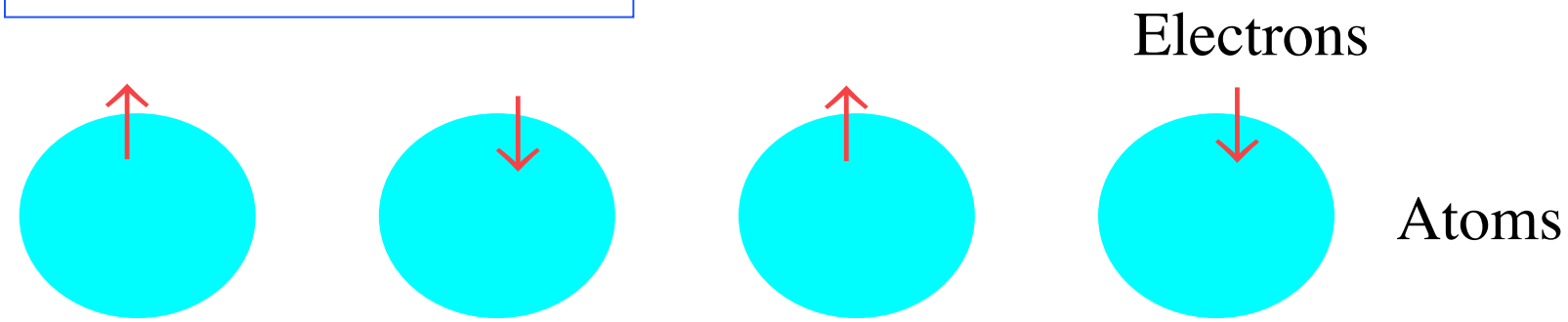

Mott insulators

MnO, FeO, CoO, Mn_3O_4, Fe_3O_4,
NiO, CuO

Insulators due to the Coulomb interaction

(Note: Antiferromagnets such as MnO and NiO are not Mott insulators in the strict sense.)

On-site Coulomb Interaction

Coulomb interaction

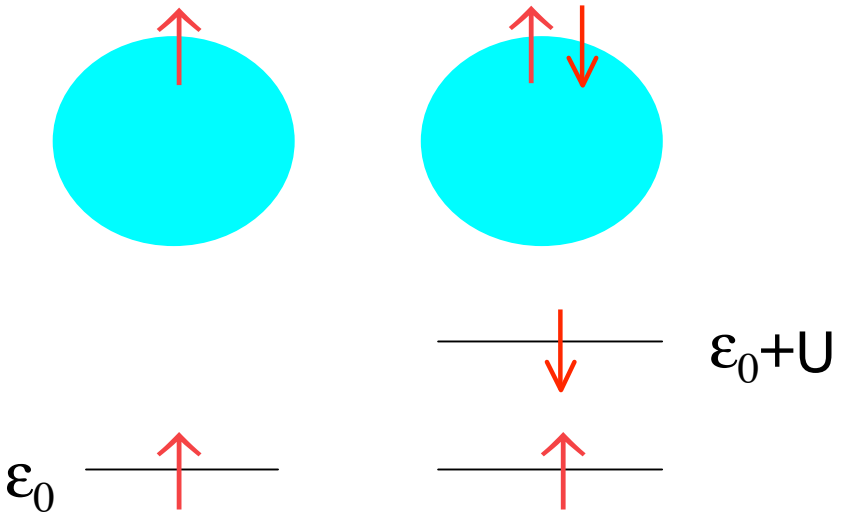

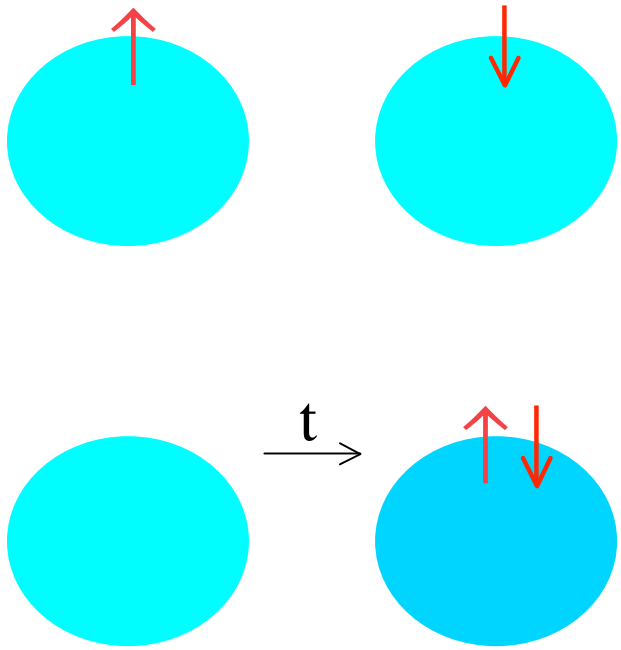

U >> t → Insulator

Gap in the Hubbard Model

Hartree-Fock theory (Half-filling)

AF Gap $\Delta = Um$ $\quad \Delta \sim t\, e^{-2\pi t/U}$ $\quad d = 1, 3$

$\sim t\, e^{-2\pi (t/U)^{1/2}}$ $\quad d = 2$

1D Hubbard model

		U << t	U >>t
Hubbard gap	Δ	$(16/\pi)\sqrt{tU}\,e^{-\pi/(2U)}$	U
Spin-wave velocity	$2v_s/\pi = J$	$(4t/\pi)(1-U/4\pi t)$	$4t^2/U$

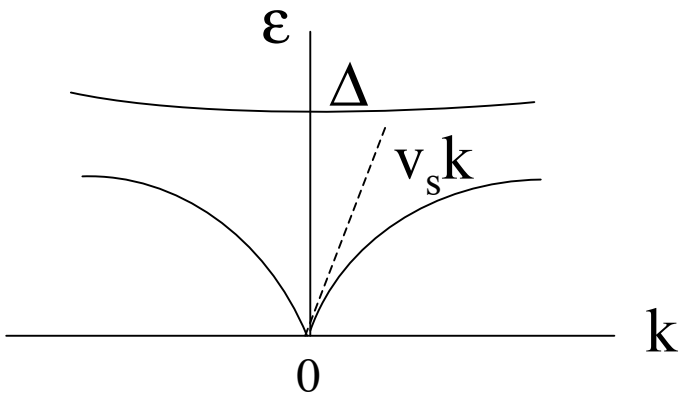

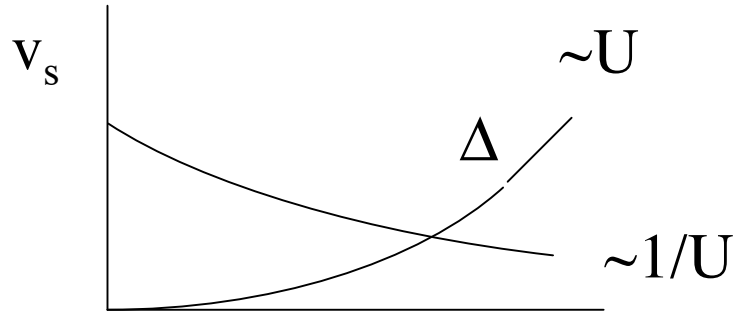

$Cu\text{-}O_2$ Model and Hubbard Model

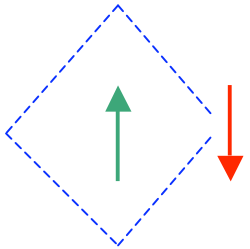

$Cu\text{-}O_2$ model
(d-p model)

Zhang-Rice singlet

Mixed state of d and p

t-J model

Hubbard model

U >> t

$$H = -t\sum_{\langle ij\rangle\sigma}(c^{+}_{i\sigma}c_{j\sigma} + h.c.) + J\sum_{\langle ij\rangle} S_i \cdot S_j$$

$$H = -t\sum_{\langle ij\rangle\sigma}(c^{+}_{i\sigma}c_{j\sigma} + h.c.) + U\sum_{i} n_{i\uparrow}n_{i\downarrow}$$

$t_{pd} \ll U_d\text{-}(\varepsilon_p - \varepsilon_d)$
$t_{pd} \ll \varepsilon_p - \varepsilon_d$
$\varepsilon_p - \varepsilon_d \ll U_d$

$\varepsilon_p - \varepsilon_d \sim 0(t_{pd})$

5. Variational Monte Carlo method

適当な波動関数の期待値をモンテカルロ法により計算する

Gutzwiller関数　$\psi_G = P_G \psi_0$

ψ_0 ：試行関数　フェルミ球、反強磁性、超伝導

$$P_G = \prod_j \left(1-(1-g)n_{j\uparrow}n_{j\downarrow}\right)$$　Gutzwiller演算子

$$0 \le g \le 1$$

パラメータgによりオンサイトの相関を制御する

weight g
Coulomb +U

weight 1

変分モンテカルロ法

Normal state ψ_0 Slater 行列式

$$\psi_0 = \sum_I a_I \psi_I$$

ψ_I ： 実空間での粒子の配置

波数 $k_1, k_2, \ldots, k_n$ 座標 $j_1, j_2, \ldots, j_n$ を↑粒子が占めている時

$$\det D_\uparrow = \begin{vmatrix} e^{ik_1 j_1} & e^{ik_1 j_2} & & e^{ik_1 j_n} \\ & & & \\ e^{ik_n j_1} & e^{ik_h j_2} & & e^{ik_n j_n} \end{vmatrix}$$

Slater 行列式

ウェイト $a_I = \det D_\uparrow \det D_\downarrow$

粒子の配置の総数は大きな数 → モンテカルロ法

モンテカルロアルゴリズム

期待値

$$\langle \psi Q \psi \rangle = \sum_{mn} a_m a_n \langle \psi_m Q \psi_n \rangle = \sum_m \frac{a_m^2}{\sum_l a_l^2} \sum_n \frac{a_n}{a_m} \langle \psi_m Q \psi_n \rangle$$

ψ_m の出現確率が $P_m = \dfrac{a_m^2}{\sum_l a_l^2}$ に比例するようにサンプルを生成すると

$$\langle \psi Q \psi \rangle = \frac{1}{M} \sum_m \left(\sum_n \frac{a_n}{a_m} \langle \psi_m Q \psi_n \rangle \right) \qquad m = 1, \mathrm{L}\ , M$$

Metropolis法　　ψ_j の次に ψ_n を生成した時（例えば、どれかの電子を動かす）

$R = |a_n|^2 / |a_j|^2 \geq \xi$ なら ψ_n を採用

$< \xi$ ψ_j のまま

ξ: 一様乱数　　$0 \leq \xi < 1$

$\langle \psi_m Q \psi_n \rangle$ の計算には余因子展開を使うとcpu時間を稼げる

超伝導状態の波動関数

$$\Psi_s = P_N P_G \psi_{BCS}$$

$$\psi_{BCS} = \prod_k (u_k + v_k c_{k\uparrow}^{+} c_{-k\downarrow}^{+})|0\rangle$$

P_N: 電子数をN個に固定

$$\Psi_s = P_G P_N \exp\left(\sum_k \frac{v_k}{u_k} c_{k\uparrow}^{+} c_{-k\downarrow}^{+}\right)|0\rangle$$

$$= P_G \left(\sum_k \frac{v_k}{u_k} c_{k\uparrow}^{+} c_{-k\downarrow}^{+}\right)^{N/2}|0\rangle$$

$$= P_G \left(\sum_k a_{ij} c_{i\uparrow}^{+} c_{j\downarrow}^{+}\right)^{N/2}|0\rangle$$

$$a_{ij} = \frac{1}{V}\sum_k \frac{v_k}{u_k} e^{ik\cdot(R_i - R_j)}$$

♠ 一般のペアー状態は、近藤さんのレクチャーにあるように、一つのSlater行列式では書けないが、BCS状態は一体近似をしているので、行列式で書くことができる。

$N_\uparrow = N_\downarrow$ の時

↑電子が$i_1, i_2, .. i_{N/2}$; ↓電子が$j_1, j_2, .. j_{N/2}$にいる時、ウェイトは行列式

$$\begin{vmatrix} a_{i_1 j_1} & \cdots & a_{i_1 j_{N/2}} \\ \vdots & & \\ a_{i_{N/2}} & \cdots & a_{i_{N/2} j_{N/2}} \end{vmatrix}$$

で与えられ、normal stateと同様に計算できる。

Superconducting state

$$\psi_{CdS} = P_G \prod_k (u_k + v_k c^+_{k\uparrow} c^+_{-k\downarrow})|0\rangle$$

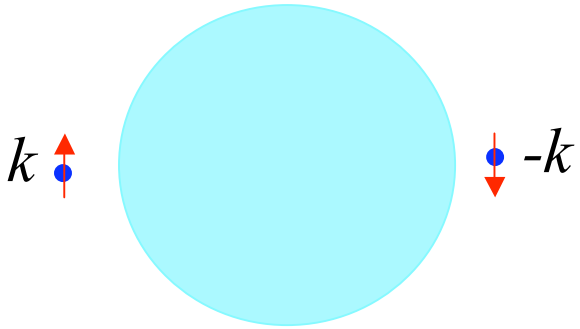

Gutzwiller Projection P_G

To control the on-site strong correlation

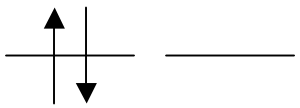

Weight g
Coulomb +U

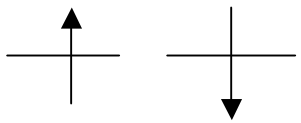

Weight 1
Parameter 0<g<1

Equivalent
to
RVB state (Anderson)

Superconducting condensation energy

SC Condensation energy

$$\Delta E_{SC} = \Omega_n - \Omega_s = \int_0^{T_c} (S_n - S_s)\,dT$$

$$= \int_0^{T_c} (C_s - C_n)\,dT$$

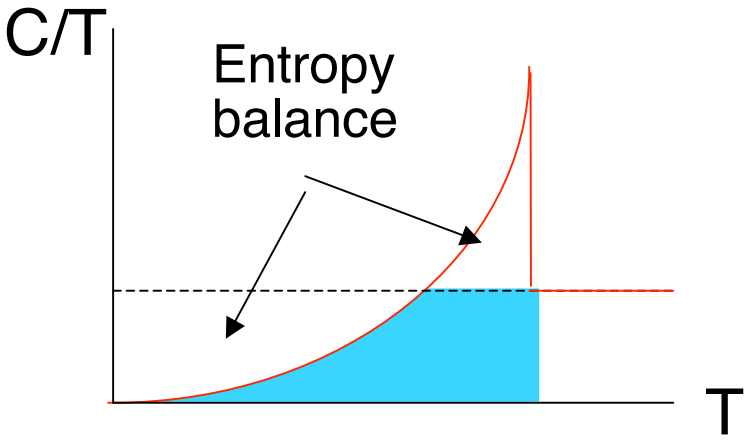

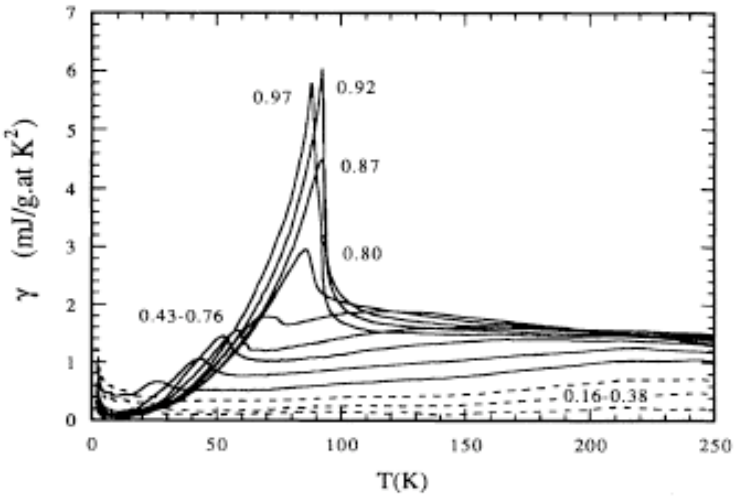

FIG. 4. Electronic specific heat coefficient $\gamma(x,T)$ vs T for $YBa_2Cu_3O_{6+x}$ relative to $YBa_2Cu_3O_6$. Values of x are 0.16, 0.29, 0.38, 0.43, 0.48, 0.57, 0.67, 0.76, 0.80, 0.87, 0.92, and 0.97.

Loram et al. PRL 71, 1740 ('93)

optimally doped YBCO

SC Condensation energy
~ 0.2 meV

Evaluations in the superconducting state

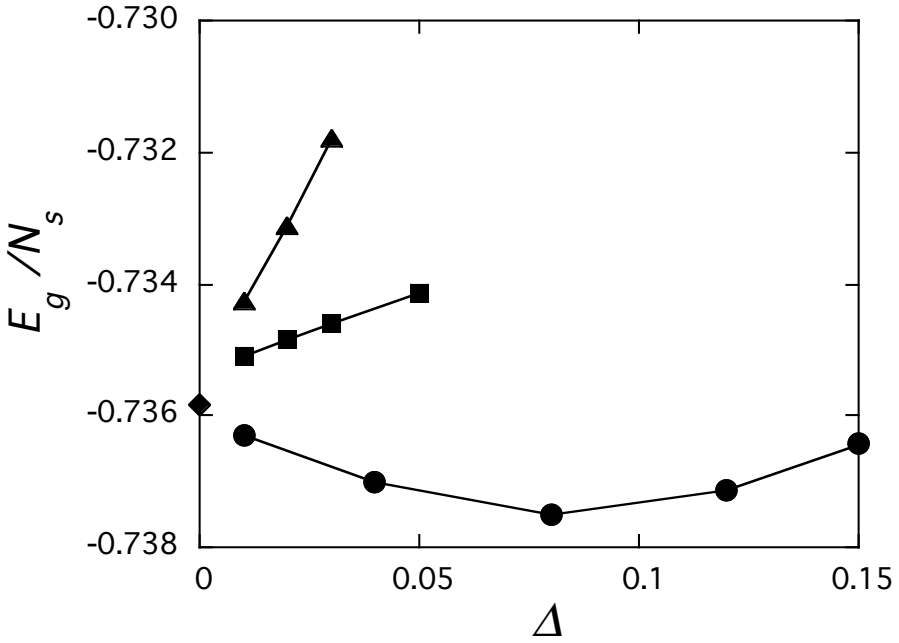

K. Yamaji et al., Physica C304, 225 (1998)
T. Yanagisawa et al.,
Phys. Rev. B67, 132408 (2003)

Variational Monte Carlo method

10x10 Hubbard model U= 8

T. Nakanishi et al. JPSJ 66, 294 (1997)

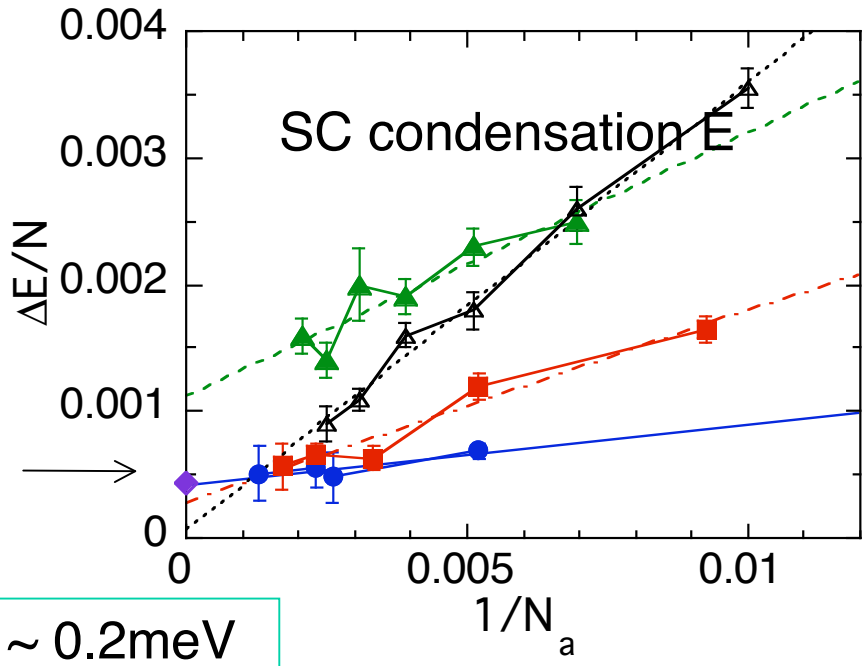

YBCO

$E_{cond} \sim 0.2meV$

Condensation Energy for d-p model

Condensation energy

$E_{cond} \sim 0.00038 t_{dp}$
$= 0.56$ meV/site

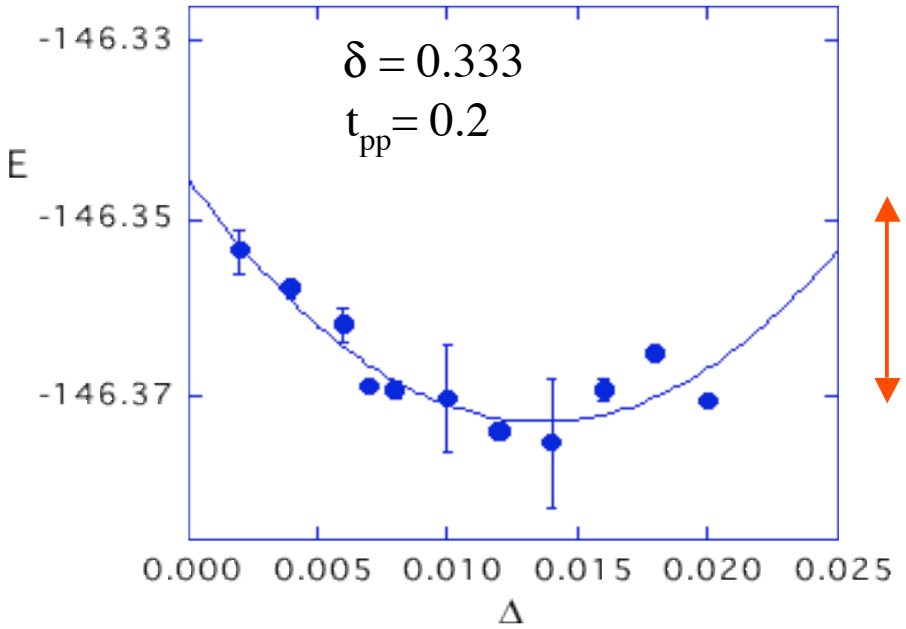

2D d-p model
6x6 and 8x8

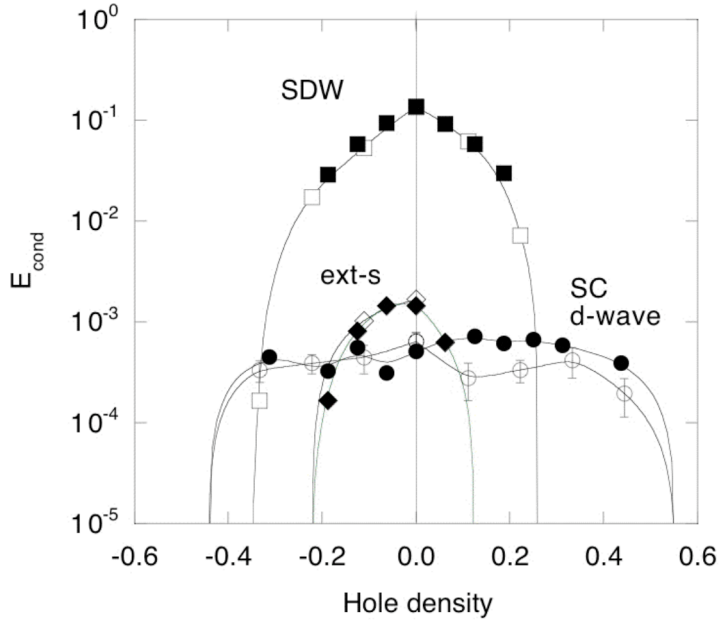

T.Yanagisawa et al., PRB64, 184509 ('01)

Superconductivity and Antiferromagnetism

Competition

Size dependence of
SC condensation energy

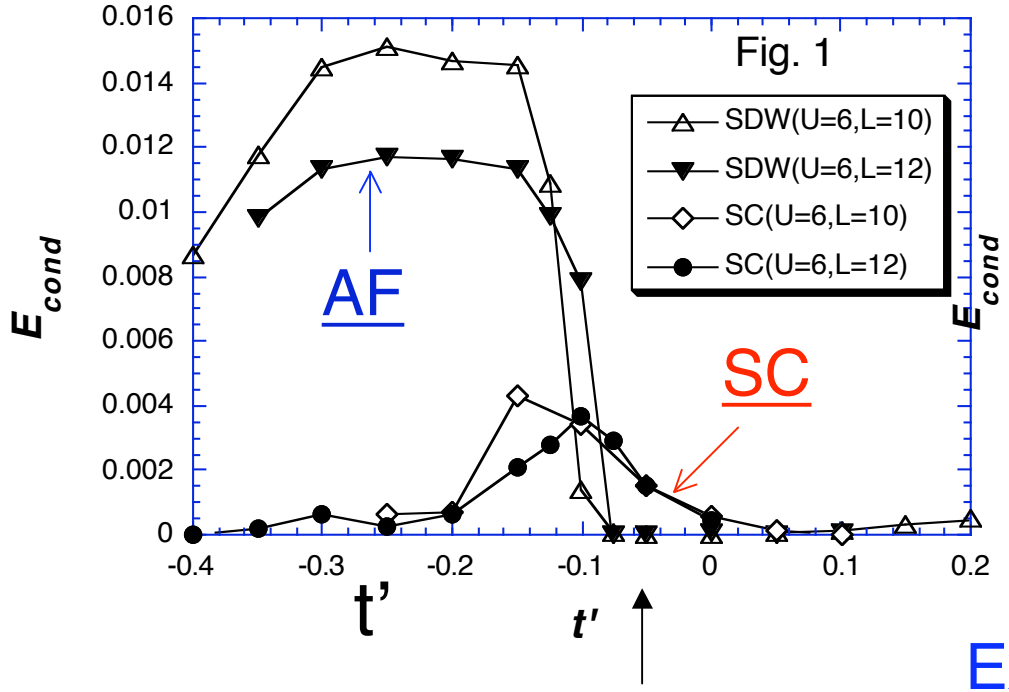

Pure d-wave SC

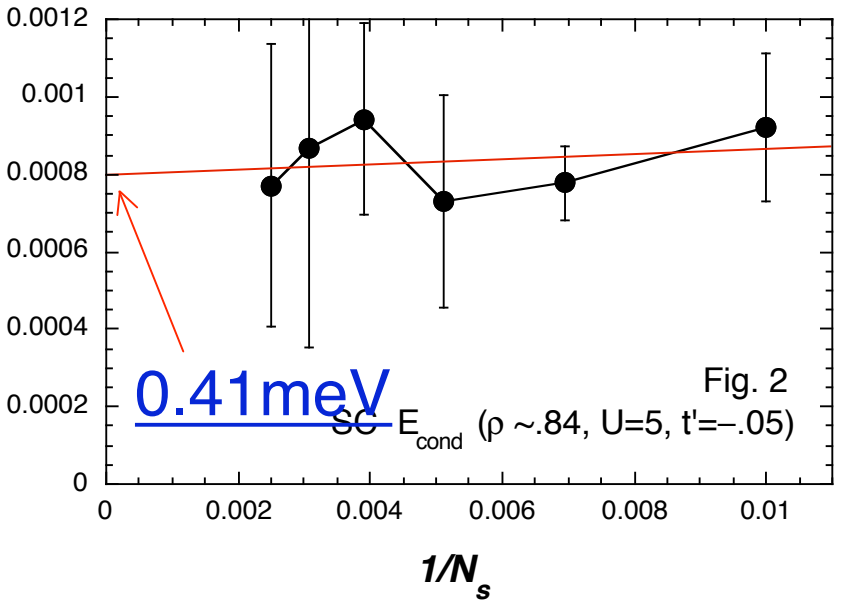

Experiments

0.26 meV/site (critical field H_c)

0.17~0.26 (C/T)

6. Stripes in high-Tc cuprates

- Vertical stripes for x > 0.05
- Diagonal stripes for x < 0.05

AF coexists with SC?

Neutron scattering

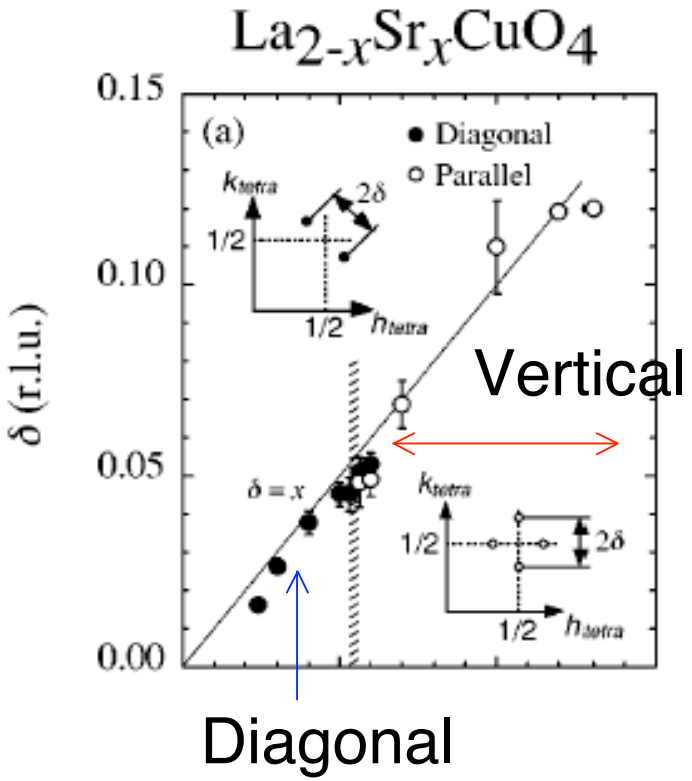

M.Fujita et al. Phys. Rev.B65,064505('02)

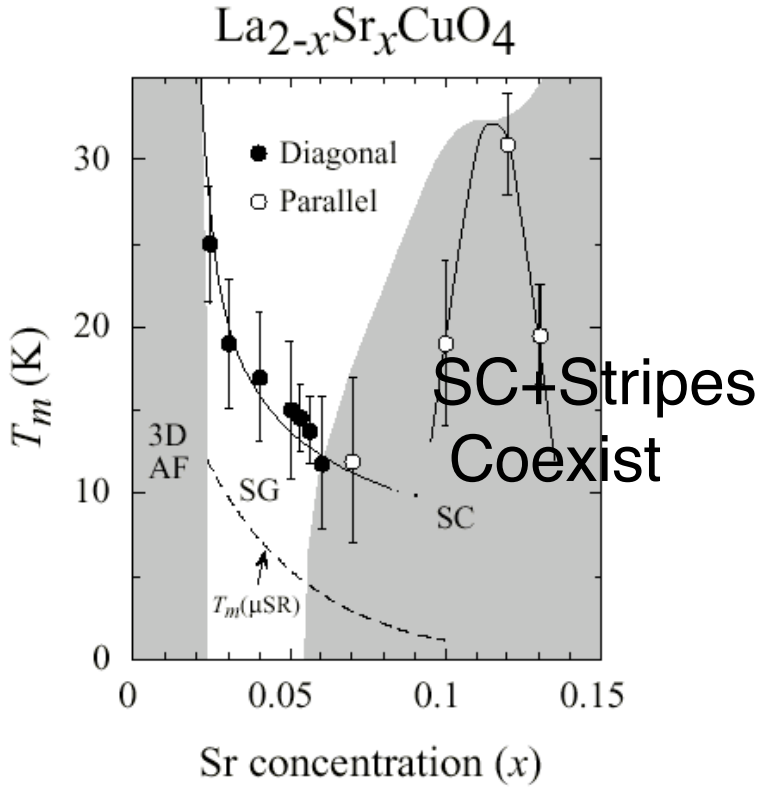

S.Wakimoto et al. PRB61, 3699('00)

Vertical Stripes in the under-doped region

Vertical stripes: 8 lattice periodicity (Tranquada)

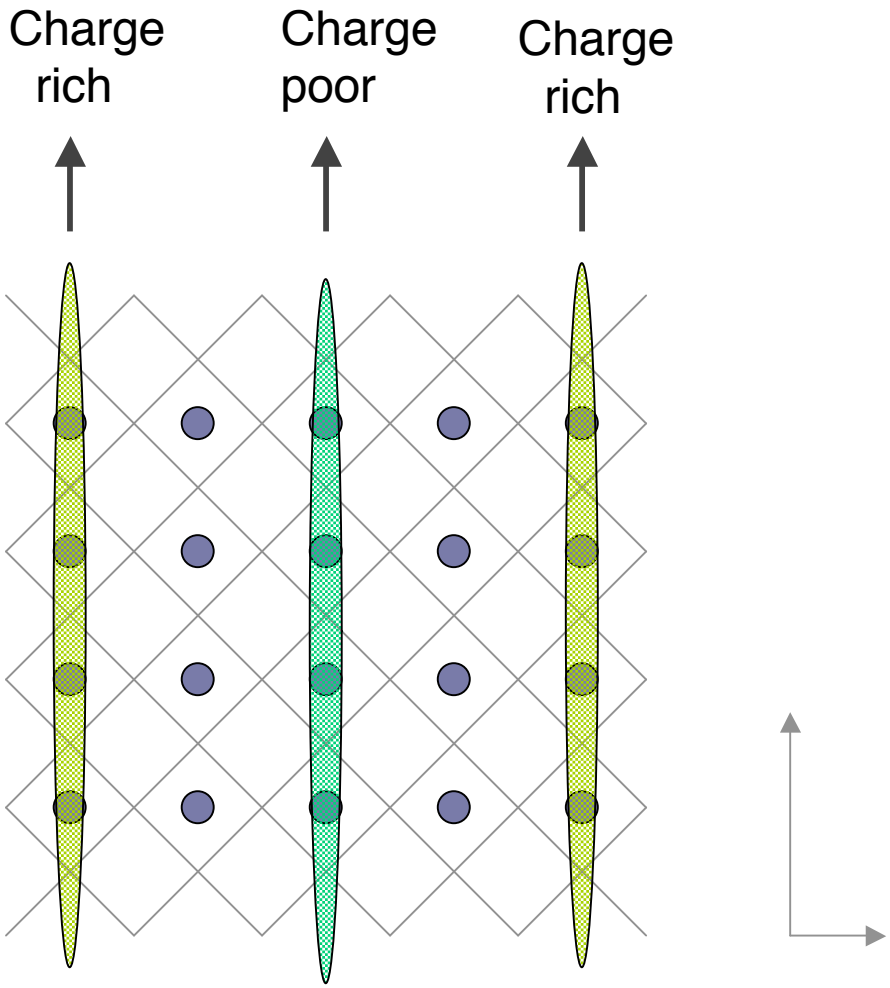

VMC

x = 1/8 3-band Hubbard

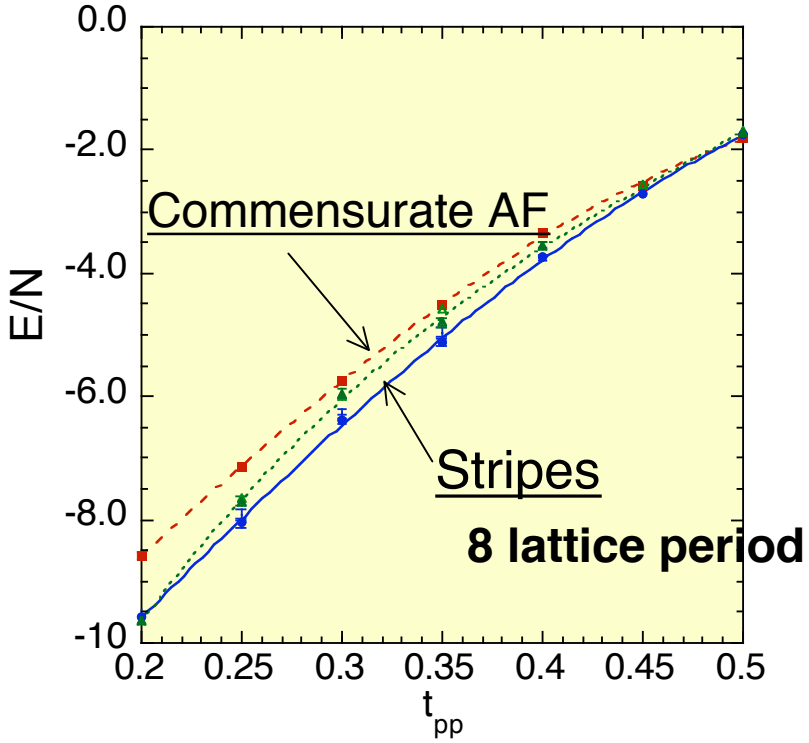

T.Y. et al., J.Phys.C14,21('02)

Stripes and Superconductivity

Compete and Collaborate

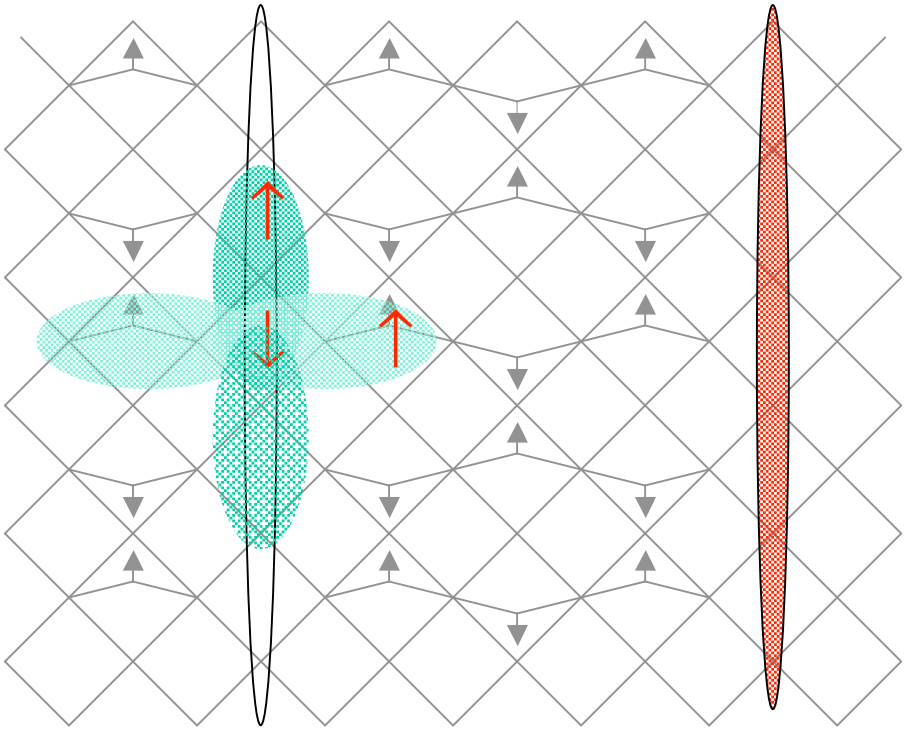

Nano-scale SC

SC coexists with stripes (AF)

Bogoliubov-de Gennes eq.

$$\begin{pmatrix} H_{ij\uparrow} + F_{ij} \\ F^{*}_{ji} - H_{ji\downarrow} \end{pmatrix} \begin{pmatrix} u^{\lambda}_{j} \\ v^{\lambda}_{j} \end{pmatrix} = E^{\lambda} \begin{pmatrix} u^{\lambda}_{i} \\ v^{\lambda}_{i} \end{pmatrix}$$

$$\alpha_{\lambda} = u^{\lambda}_{i} a_{i\uparrow} + v^{\lambda}_{i} a^{+}_{i\downarrow}$$

$$\overline{\alpha_{\lambda}} = \bar{u}^{\lambda}_{i} a_{i\uparrow} + \bar{v}^{\lambda}_{i} a^{+}_{i\downarrow}$$

Wave function

$$V_{\lambda j} = v^{\lambda}_{j} \qquad (\overline{U})_{\lambda j} = \bar{u}^{\lambda}_{j}$$

$$\psi_{SC} = P_G P_{N_e} \prod_{\lambda} \alpha_{\lambda} \bar{\alpha}^{+}_{\lambda} |0\rangle \propto P_G \left(\sum_{ij} (U^{-1}V)_{ij} a^{+}_{i\uparrow} a^{+}_{j\downarrow} \right)^{N_e/2} |0\rangle$$

Diagonal stripes in lightly doped region

Diagonal stripes are observed for

$La_{2-x}Sr_xNiO_4$
$La_{2-x}Sr_xCuO_4$
$La_{2-x-y}Nd_ySr_xCuO_4$

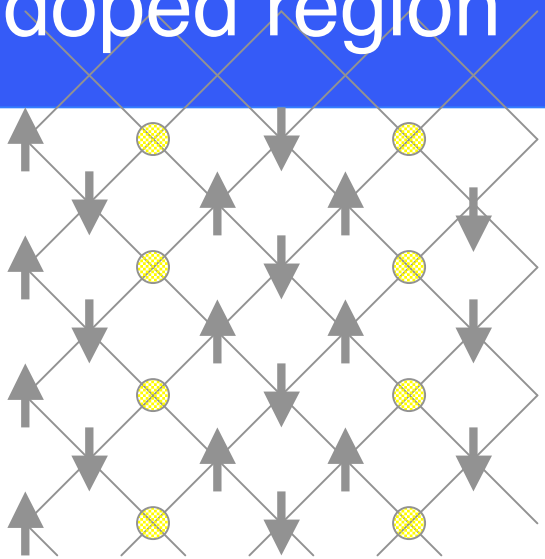

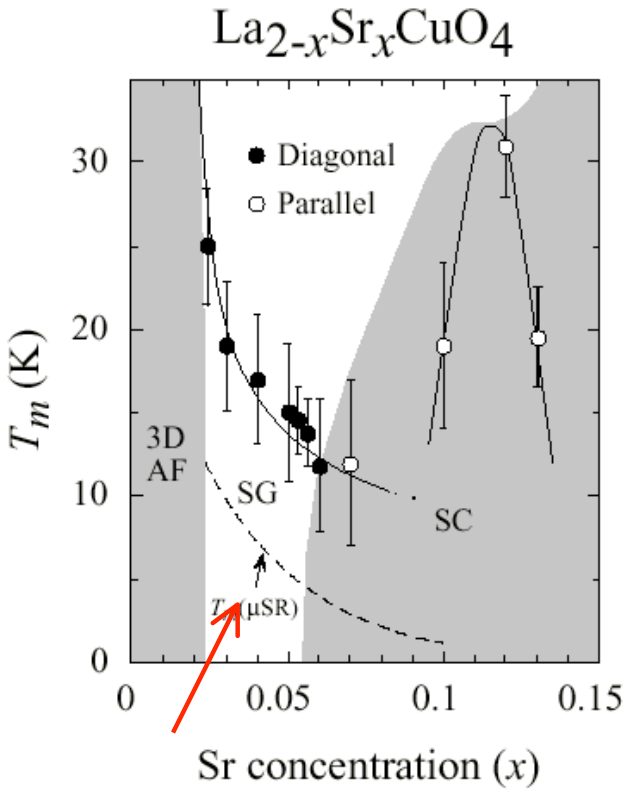

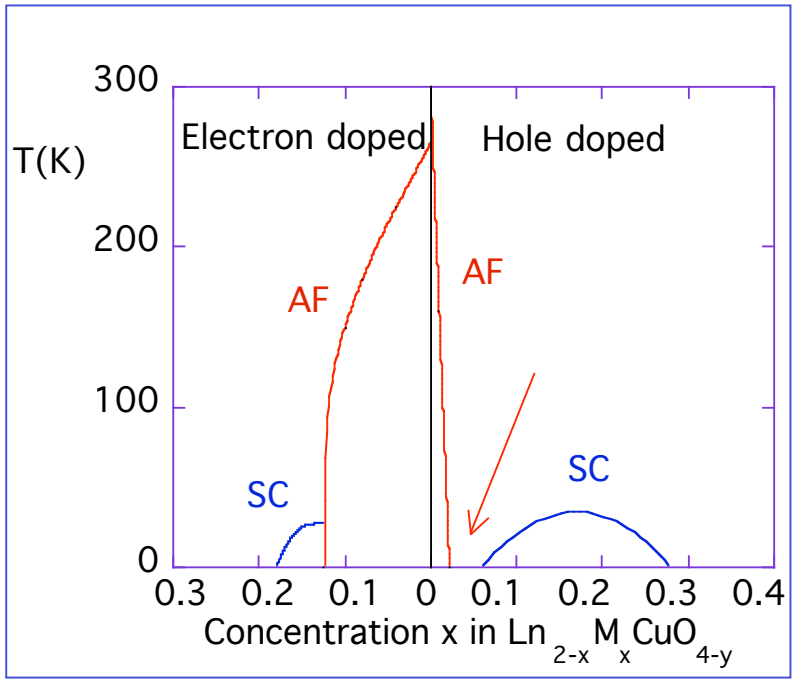

Incommensurability: Comparison with Experiments

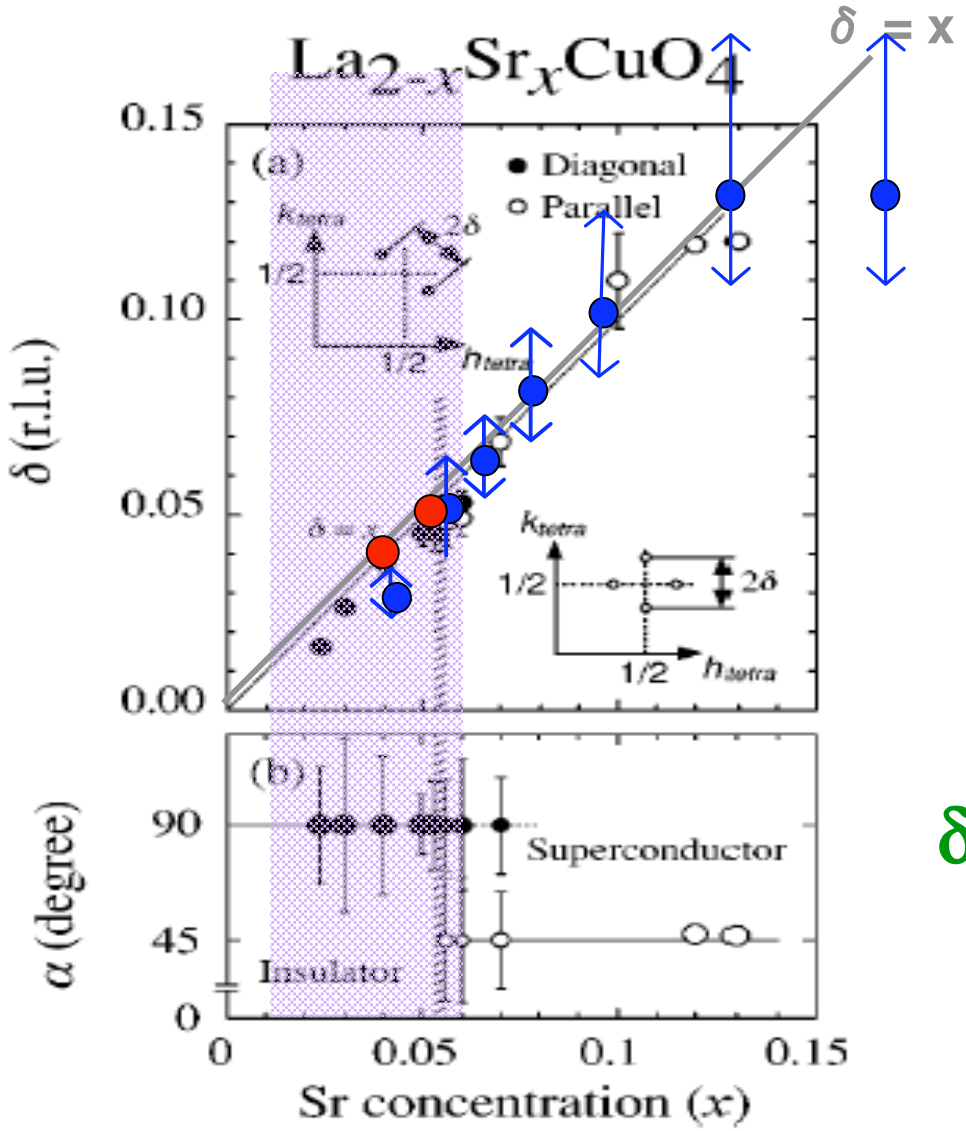

● Vertical stripes

● Diagonal stripes

U=8.0 t'= -0.2

δ can be explained by 2D Hubbard model.

Stripes and Structural transition

Structural transitions: Lattice distortions
LTT,LTO,LTLO,HTT

Stripes: suggested by Incommensurability

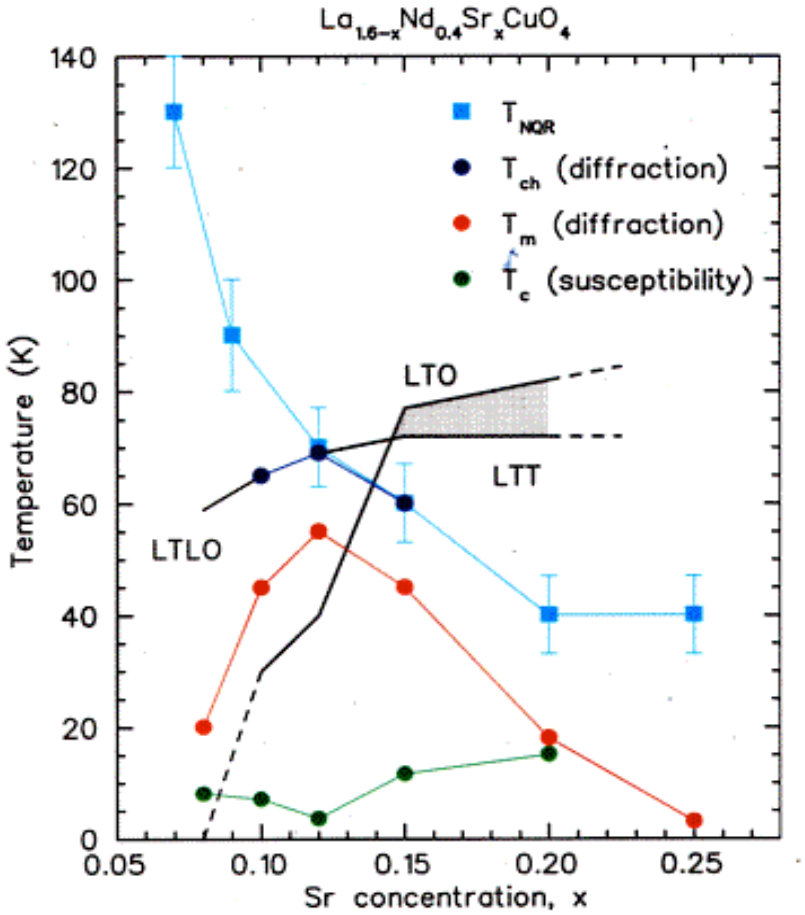

N.Ichikawa et al.
PRL85, 1738('00)

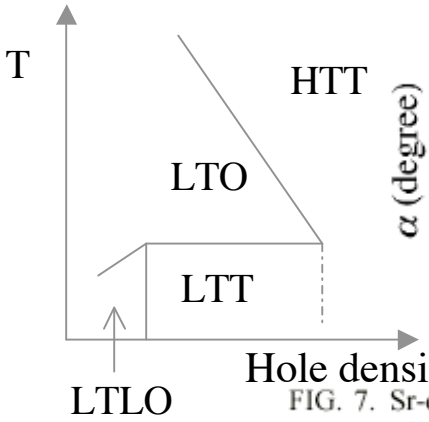

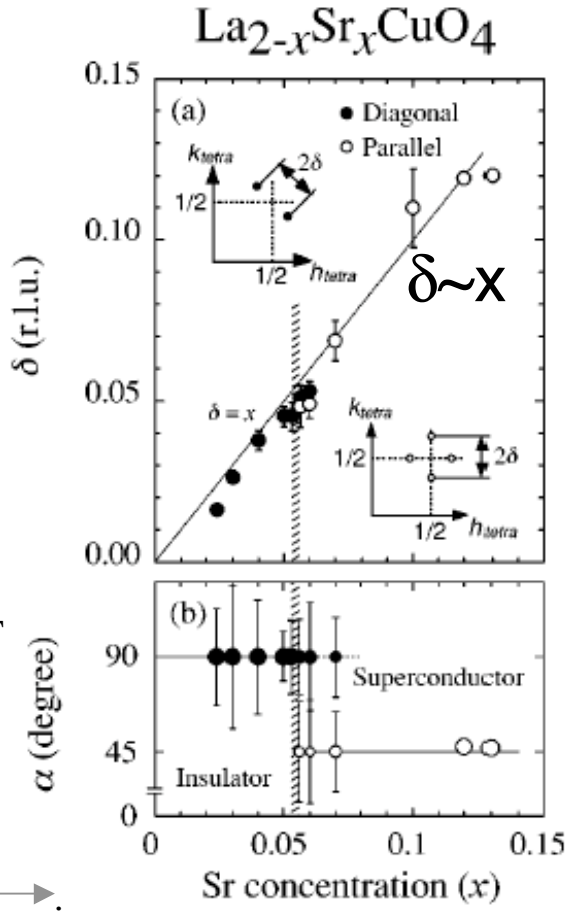

FIG. 7. Sr-concentration dependence of (a) the incommensurability δ and (b) the angle a defined in Fig. 3. Previous results for $x = 0.024$ (Ref. 11), 0.04 (Ref. 10), 0.05 (Ref. 10), 0.12 (Ref. 5), 0.1 (Ref. 15), and 0.13 (Ref. 15) are included. In both figures, the solid and open symbols represent the results for the diagonal and parallel components, respectively.

M.Fujita et al. Phys. Rev.B65,064505('02)

What happens under lattice distortions?

1. Anisotropy of the transfer integrals
   Anisotropic electronic state
   vertical stripes
   Diagonal stripes x<0.05

2. Spin-Orbit Coupling induced from lattice distortions

3. Electron-phonon interaction

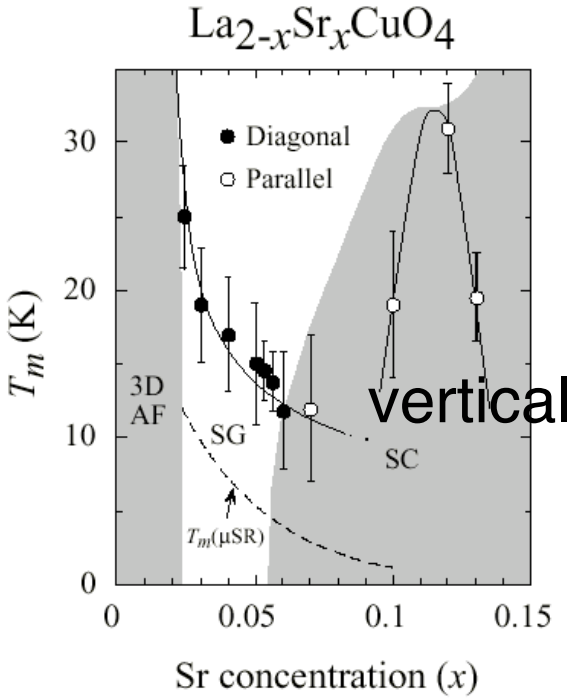

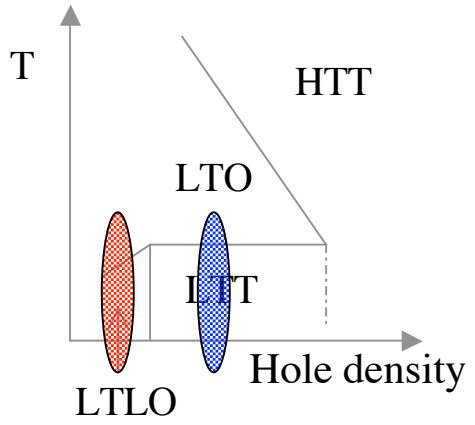

Anisotropy of the transfer integrals in LTT phase

One-band Hubbard model (Miyazaki)

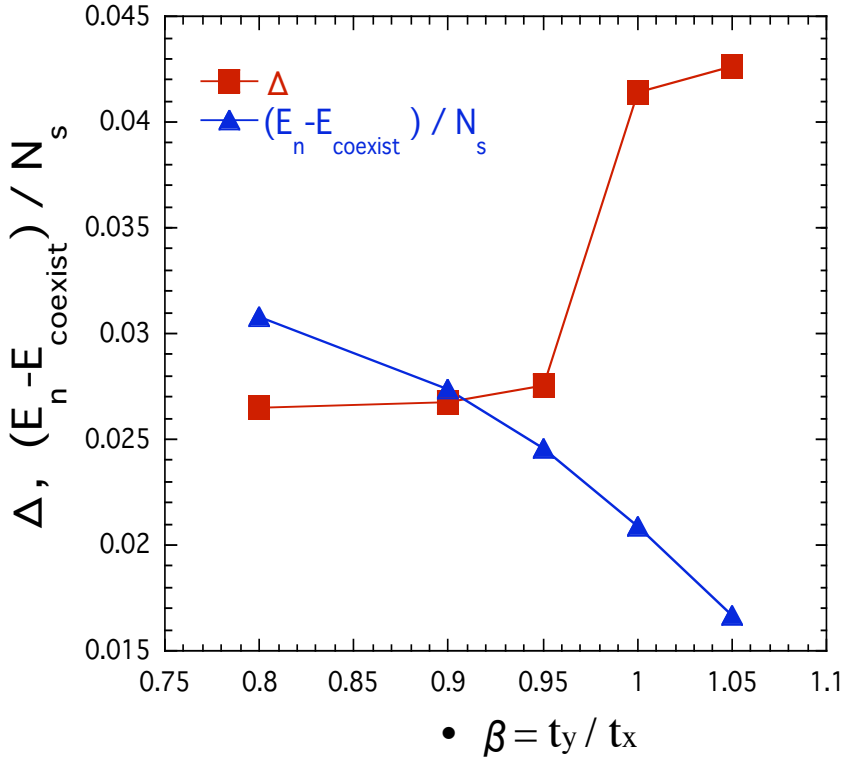

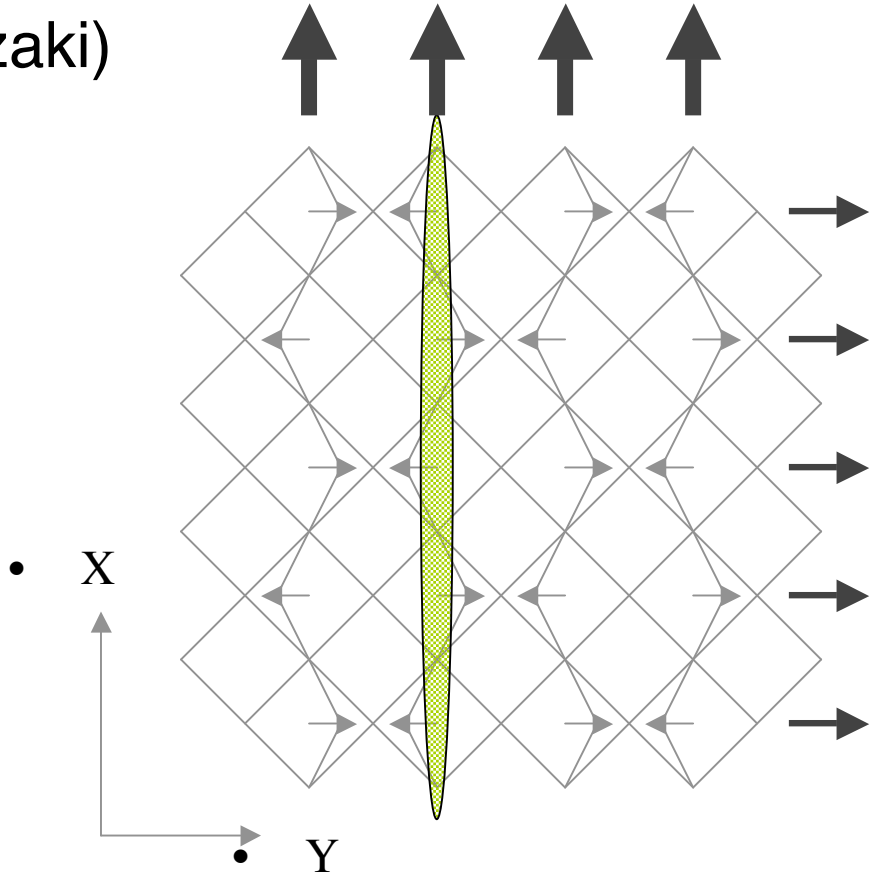

LTT structural transitions stabilize stripes.

Possible Stripe Structure 1

Mixed phase of LTT and LTLO

Stabilize stripes

M. K. Crawford et. al.

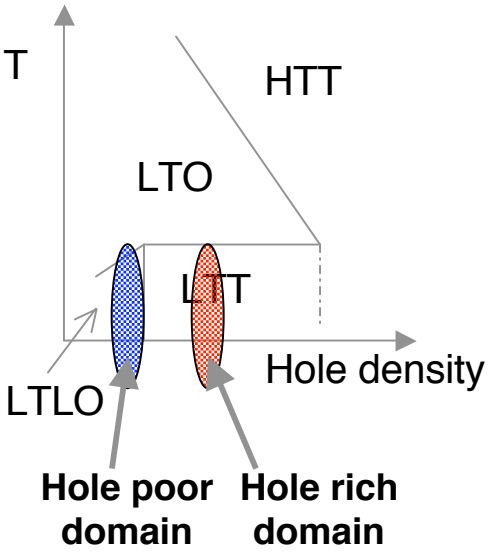

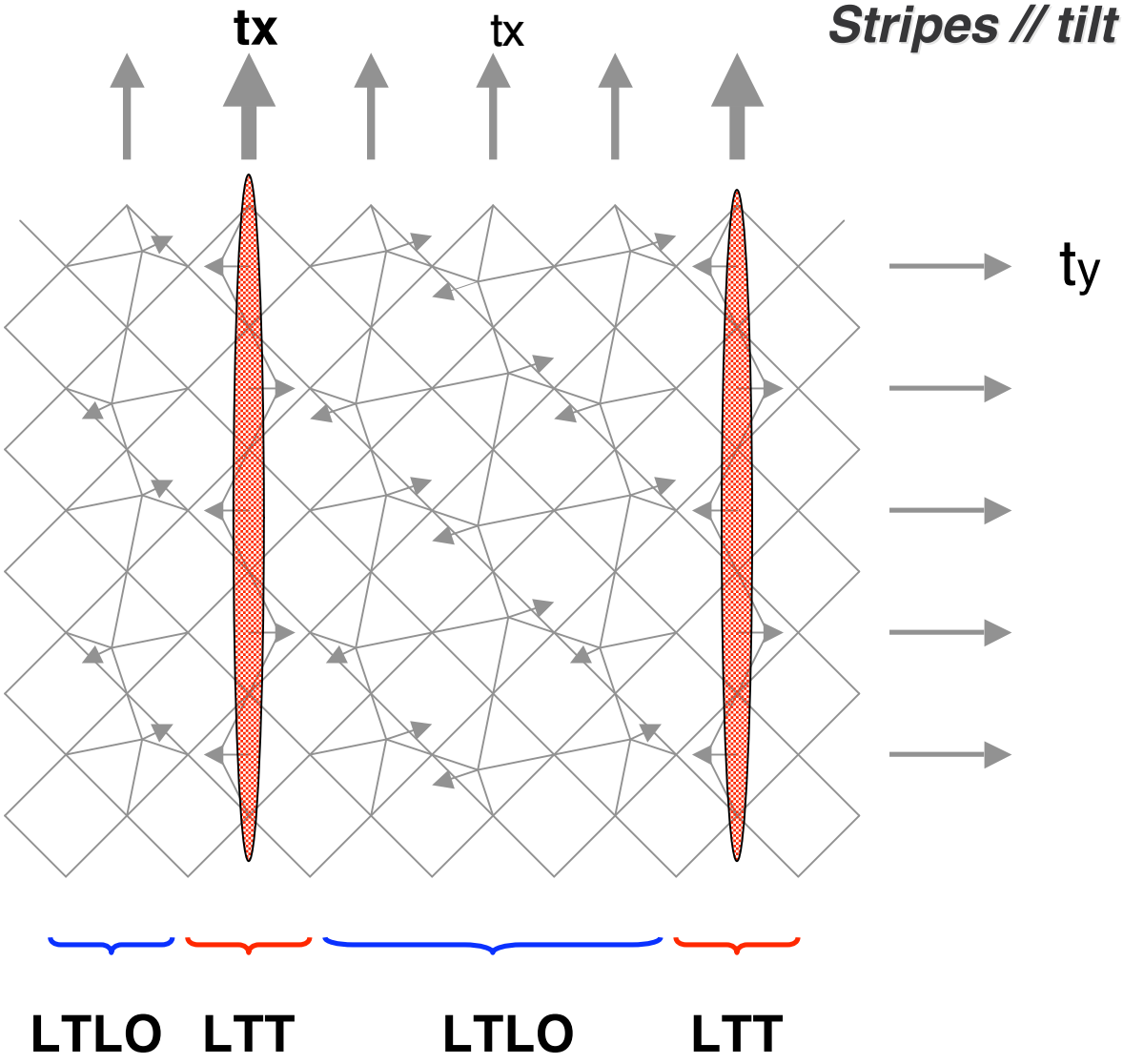

Possible Stripe Structure 2

Mixed phase of LTT and HTT

Stripes perpendicular to tilt axis

Stable

M. K. Crawford et. al.

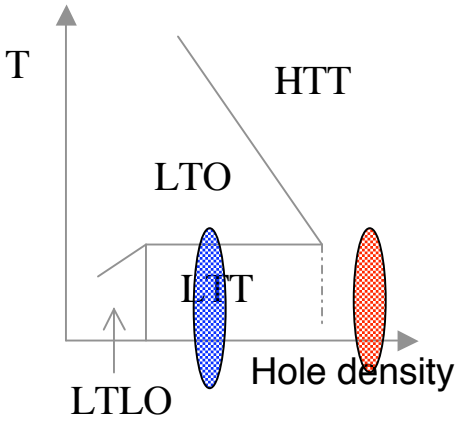

Oscillation of tilt angles

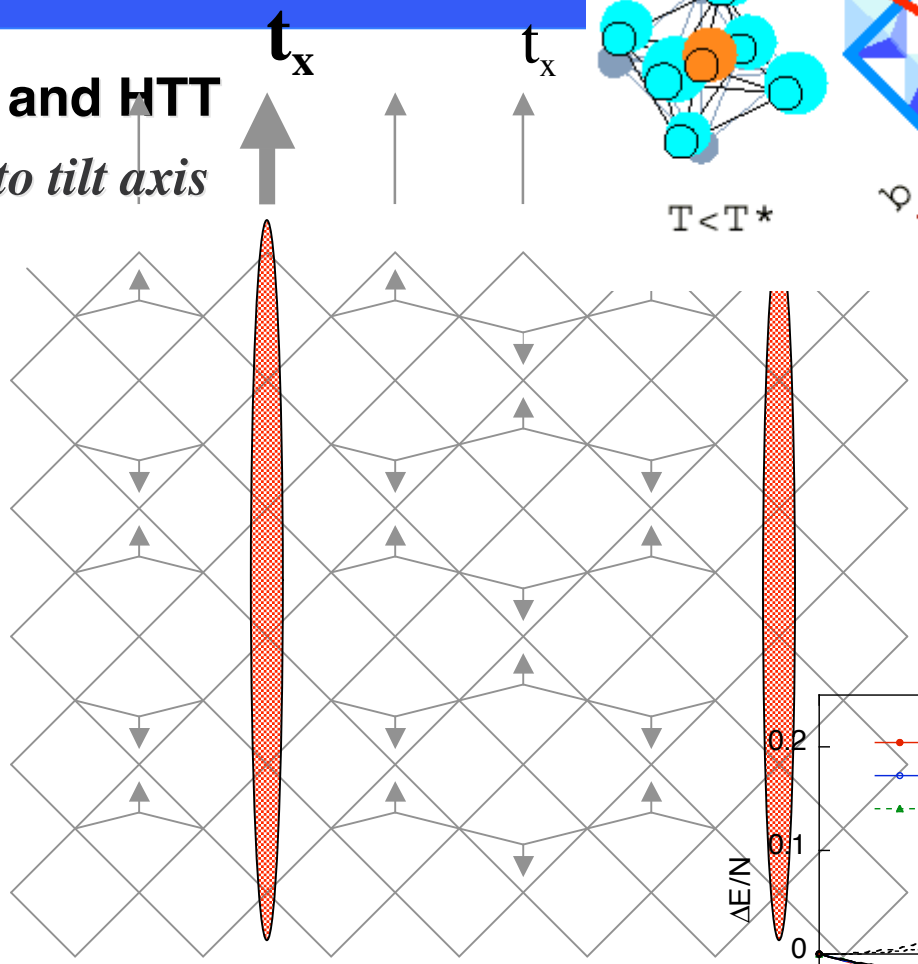

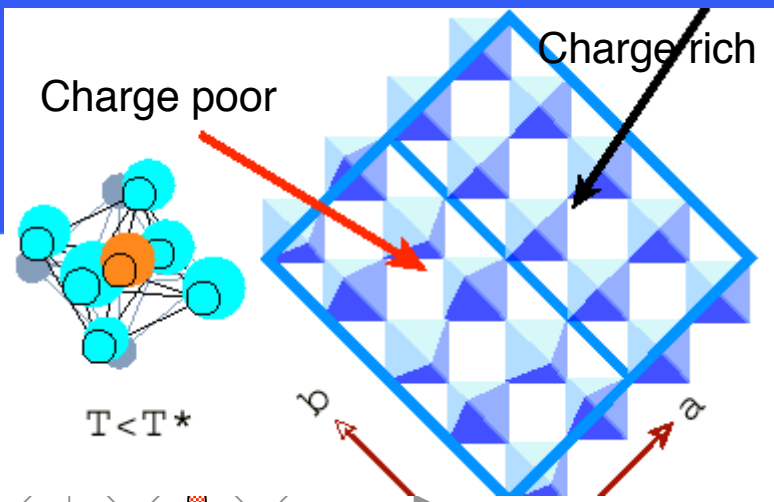

H. Oyanagi
A. Bianconi

t_y

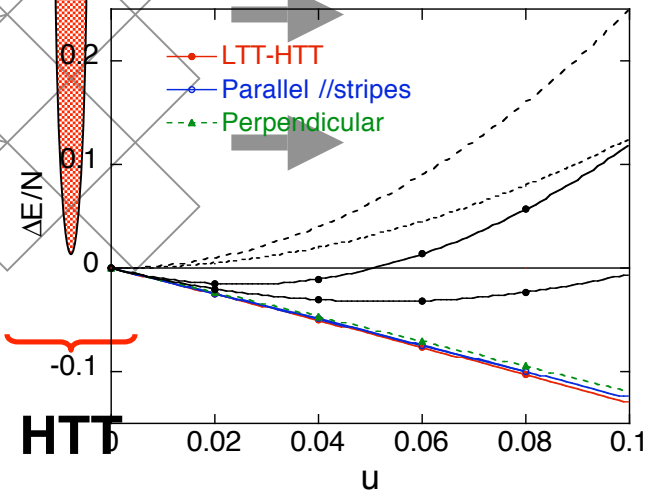

7. Spin-orbit coupling and Lattice distortion

Spin-Orbit Coupling induced by the Lattice distortion

Tilting

Friedel et al., J.Phys.Chem.Solids 25, 781 (1964)

$$\langle p_x(x-a/2,y)\uparrow|H_{dp}|d_{xz}(r)\uparrow\rangle = -t_{xz}e^{-ik_x/2\cdot a}$$

$$\langle p_y(x,y-a/2)\uparrow|H_{dp}|d_{yz}(r)\uparrow\rangle = -t_{yz}e^{-iky/2\cdot a}$$

$$H_{SO} = \xi(r)L\cdot S$$

$$\langle d_{xz}(r)\uparrow|H_{SO}|d_{yz}(r)\uparrow\rangle = -\frac{i}{2}\xi$$

$$\langle d_{yz}(r)\uparrow|H_{SO}|d_{xz}(r)\uparrow\rangle = \frac{i}{2}\xi$$

$$\langle d_{x^2-y^2}(r)\uparrow|H_{SO}|d_{yz}(r)\downarrow\rangle = \frac{i}{2}\xi$$

$$\langle d_{x^2-y^2}(r)\uparrow|H_{SO}|d_{xz}(r)\downarrow\rangle = \frac{1}{2}\xi$$

Effective iξ term for p-p transfer

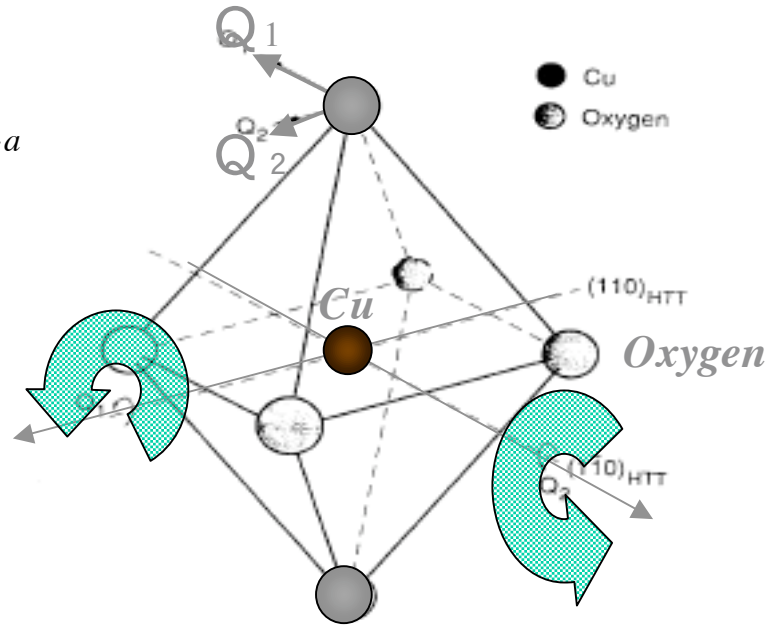

t_{xz}, t_{yz} ≠0 ~ tilt angle

Five orbitals × (↑↓):

($d_{x^2-y^2}$, d_{xz}, d_{yz}, p_x, p_y)

Dispersion in the presence of spin-orbit coupling

d-p model

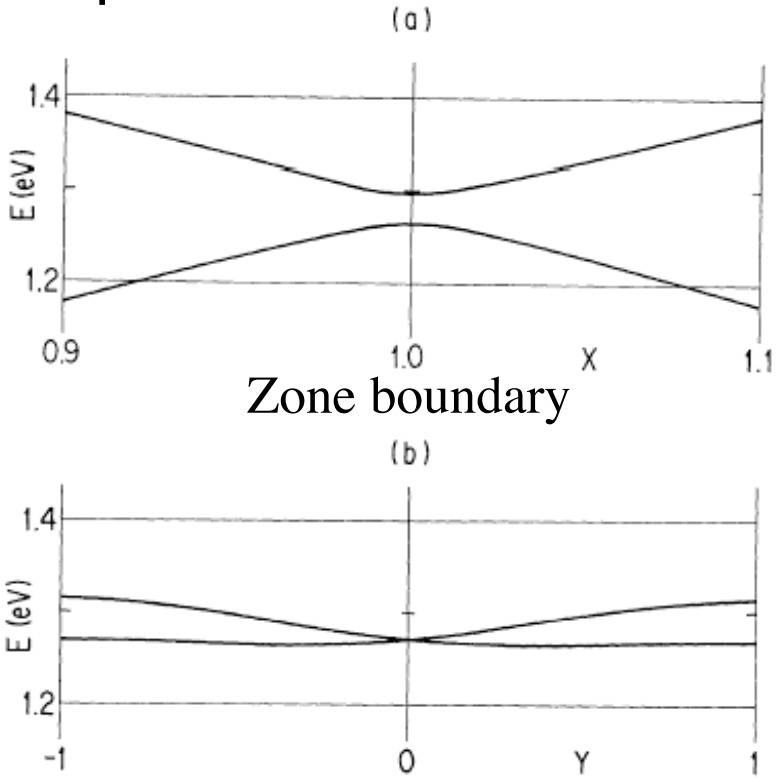

$\xi = 0.4$ (K.Yamaji, JPSJ(1988))

One-band effective model

$$H_{kin} = -\sum_{ij\sigma} (t_{ij} + ic\,\sigma\theta_{ij}) d^{+}_{i\sigma} d_{j\sigma}$$

(Bonesteal et al.,PRL68,2684('92))

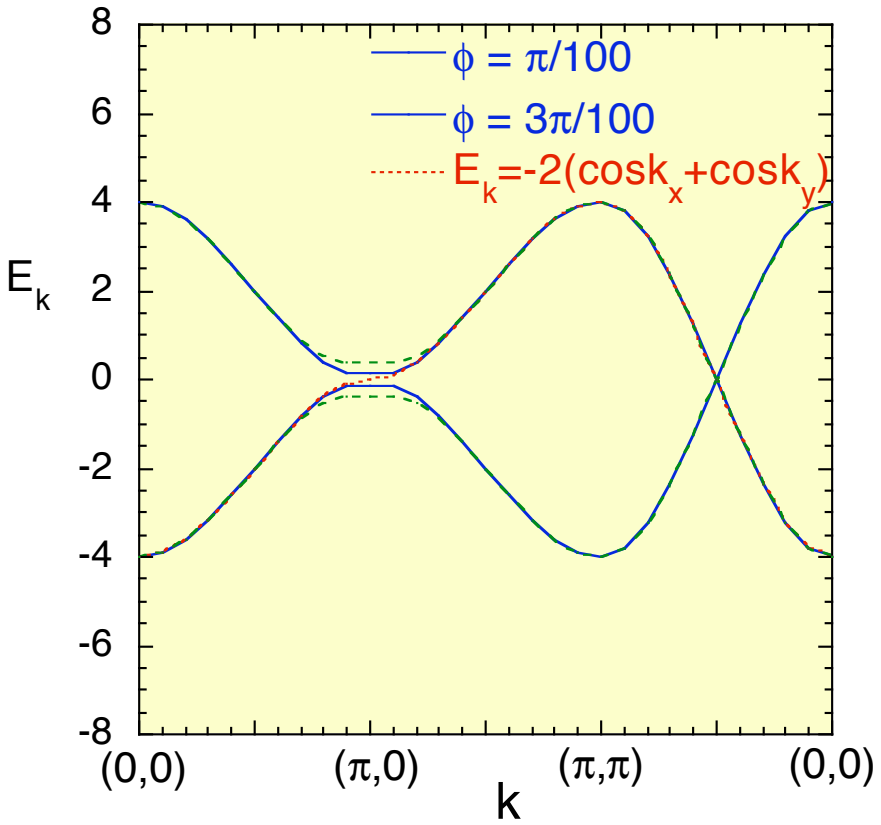

Flux state

$$E(k_x,k_y) = \pm\left| e^{i\phi/4}e^{ik_x} + e^{-i\phi/4}e^{ik_y} + e^{i\phi/4}e^{-ik_x} + e^{-i\phi/4}e^{-ik_y} \right|$$

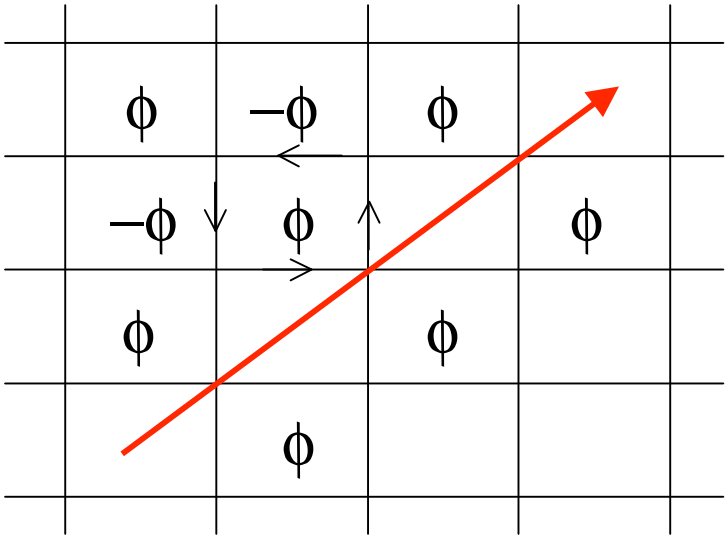

Excitation: Dirac fermion

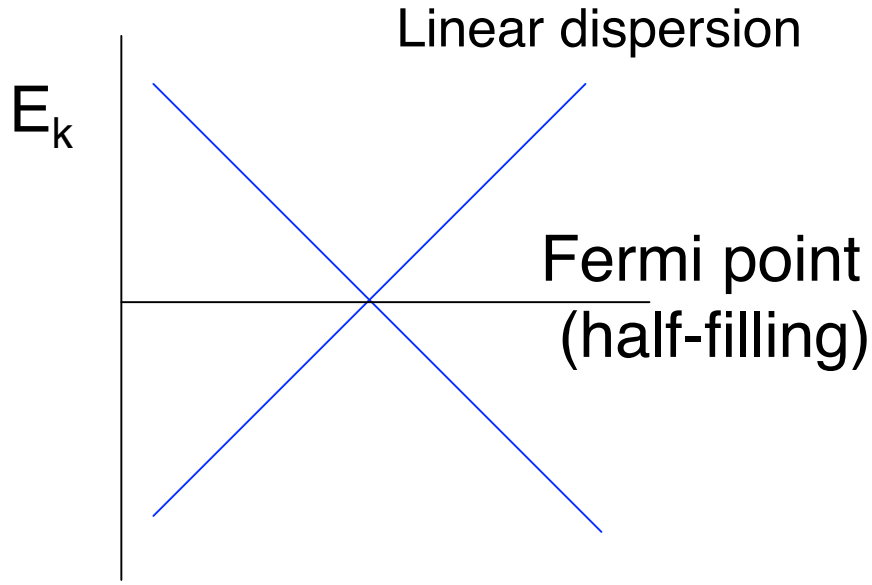

Small Fermi surface

Inhomogeneous d-density wave

Pseudo-gap in the density of states

Flux state

⟶ Pseudo-gap

An origin of pseudo-gap

Density of states

$$N_\sigma(k,\varepsilon) = -\frac{1}{\pi}\,\mathrm{Im}\,G_\sigma(k,\varepsilon+i\delta)$$

Eigenfunction $\varphi_{\sigma m}(r)$

$$H\varphi_{\sigma m}(r) = E_{\sigma m}\varphi_{\sigma m}(r)$$

$$G_\sigma(r,r',i\omega) = \sum_m \frac{\varphi_{\sigma m}(r)\varphi^*_{\sigma m}(r')}{i\omega - E_{\sigma m}}$$

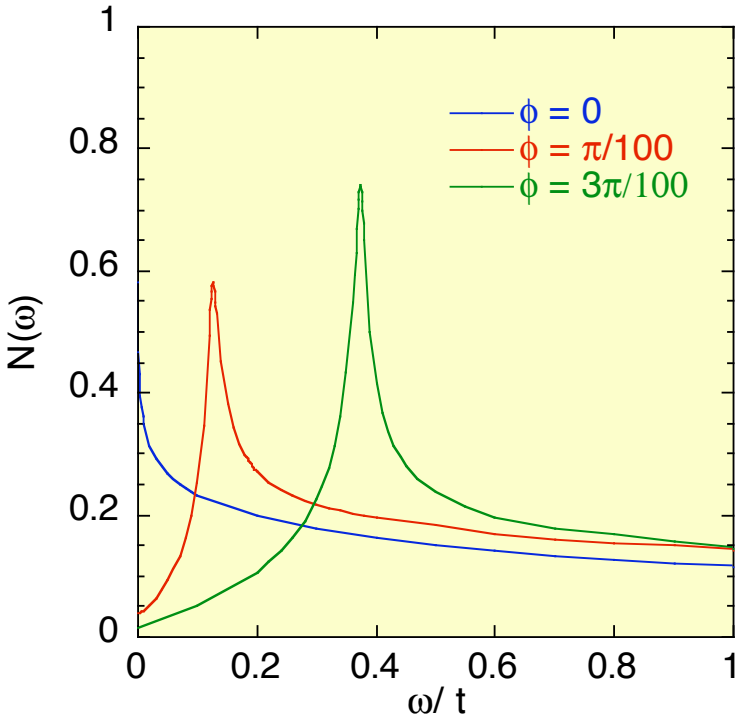

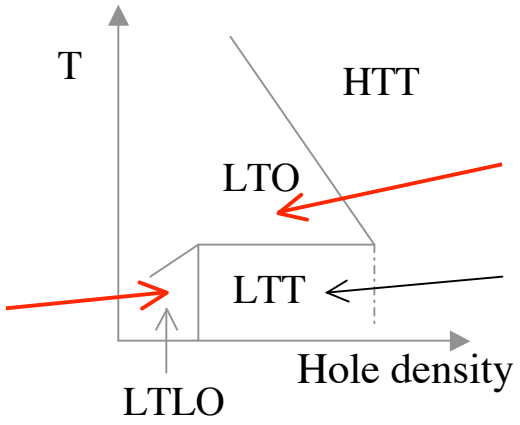

Diagonal stripes with Spin-orbit coupling

Spin-orbit coupling induces flux.

Spin-orbit coupling stabilizes the diagonal stripes.

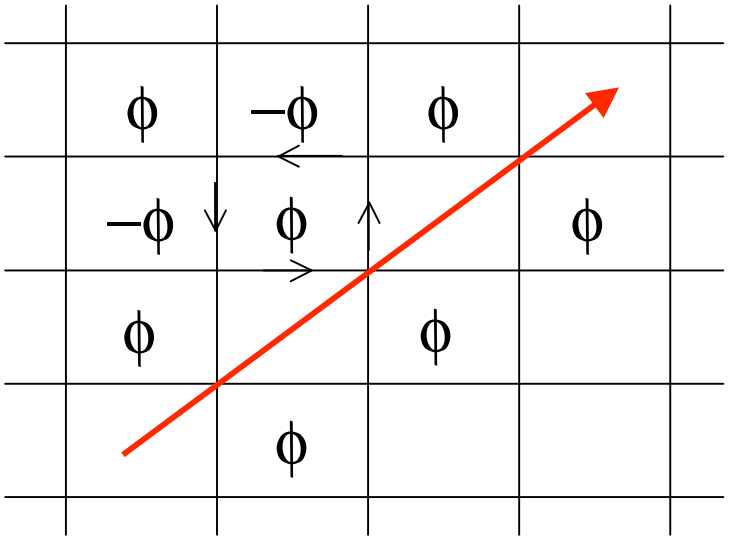

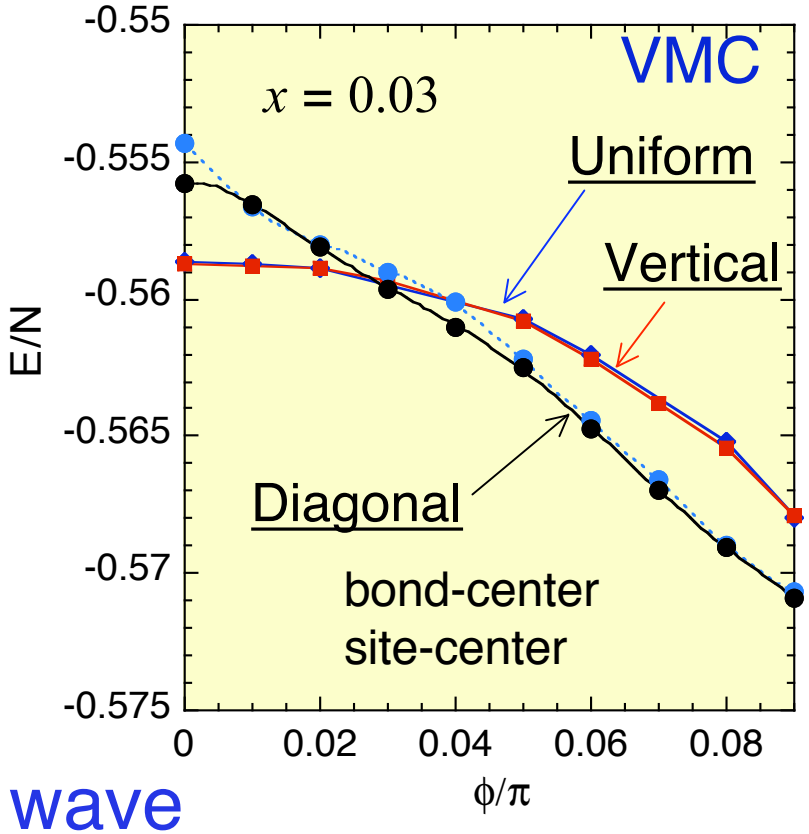

Diagonal Stripe & d-density wave

$\Phi = 4\phi$

d-density wave

d-density wave

$$i\Delta_Q Y(k) = \left\langle c^+_{k+Q\sigma} c_{k\sigma} \right\rangle \quad Q = (\pi, \pi)$$

$$Y(k) = \cos(k_x) - \cos(k_y)$$

Nayak, Phys. Rev. B62, 4880 ('00)
Chakravarty et al., PRB63, 094503 ('01)

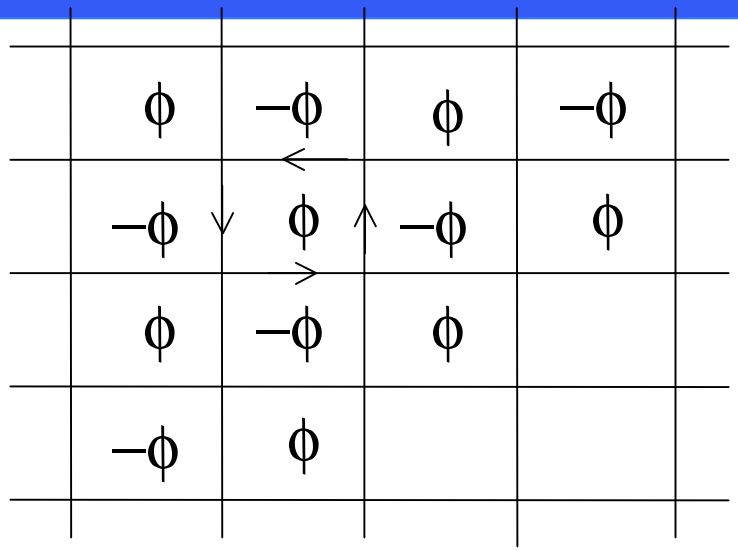

Inhomogeneous density wave

$$i\Delta_Q Y(k) = \left\langle c^+_{k+Q\sigma} c_{k\sigma} \right\rangle$$ d-symmetry

$$\Delta_{lQ_s\sigma} = \sum_k \left\langle c^+_{k+lQ_s\sigma} c_{k\sigma} \right\rangle$$ incommensurate

$Q_s = (\pi+2\pi\delta, \pi)$ vertical

$Q_s = (\pi+2\pi\delta, \pi+2\pi\delta)$ diagonal

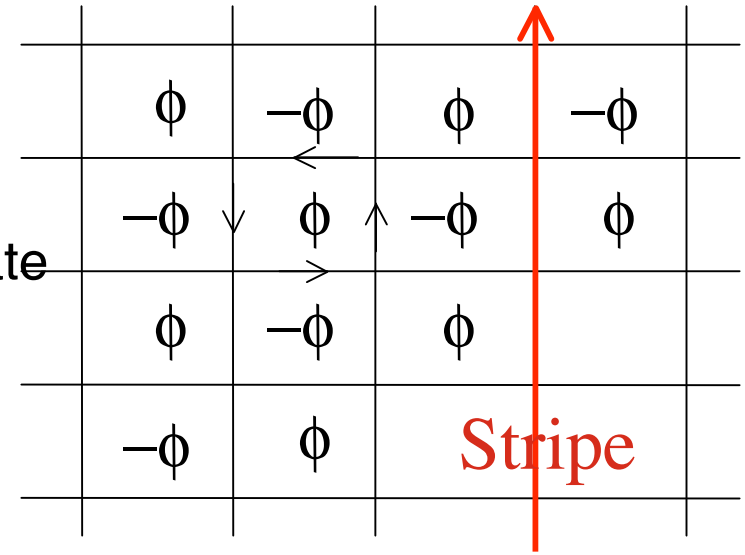

8. Summary

$$\psi_{CdS} = P_G \prod_k (u_k + v_k c^+_{k\uparrow} c^+_{-k\downarrow})|0\rangle$$

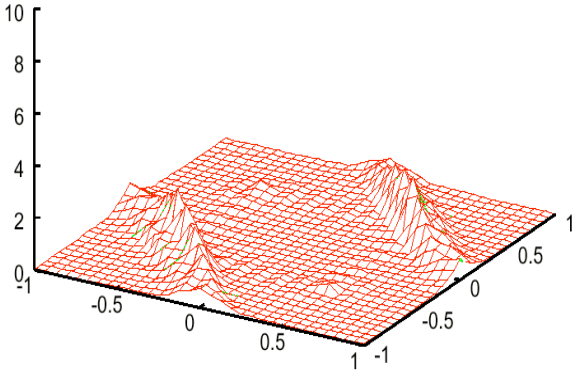

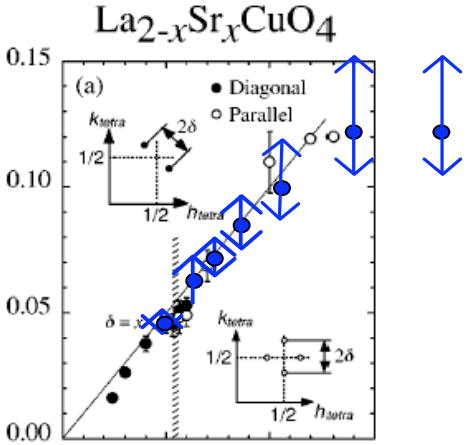

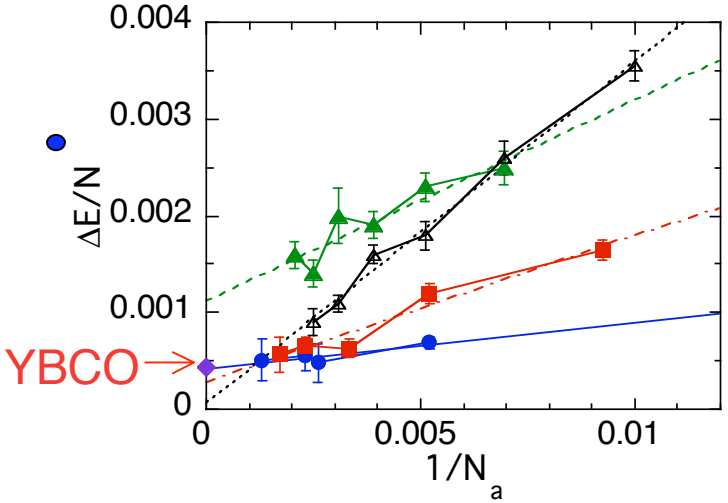

Explanation of spectra

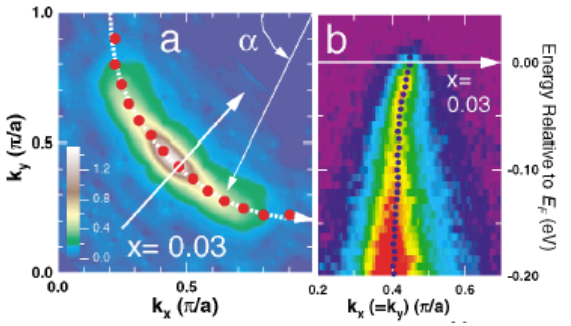

ARPES Measurements

Incommensurability Neutron scatterings

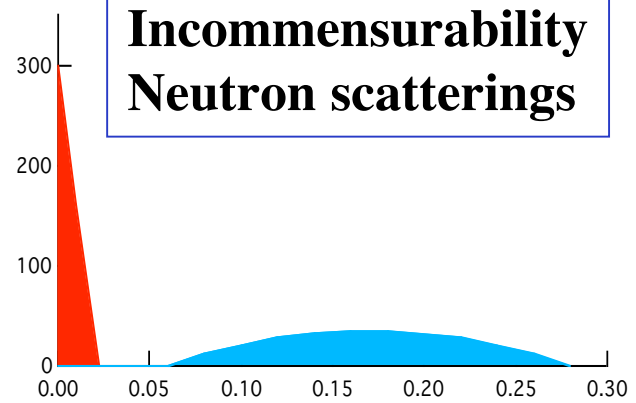

underdope

overdope

Theoretical estimate of SC condensation energy

Agreement with Exp.

$E_{cond} \sim 0.2meV$